

REPUBLIC OF TURKEY

ONDOKUZ MAYIS UNIVERSITY

INSTITUTE OF SCIENCES, SAMSUN



3D RECONSTRUCTION OF POINT CLOUDS AND SOLID MODELS FROM LIDAR AND DIGITAL STEREO IMAGES

A THESIS SUBMITTED TO THE DEPARTMENT OF GEOMATICS / SURVEYING ENGINEERING IN PARTIAL FULFILLMENT OF THE REQUIREMENTS FOR THE DEGREE OF MASTER OF SCIENCE (MSc)

PRESENTED

BY

Abu KAMARA

11210295

EXAMINATION DATE: 14.01.2015

SUPERVISED BY; ASSISTANT Prof. Dr. Sedat DOĞAN

Republic Of Turkey

Ondokuz Mayıs University Institute Of Sciences, Samsun

3D Reconstruction Of Point Clouds And Solid Models From LİDAR And Digital Stereo Images

From Jury's part 14/01/2015 examination date this work has been accepted as Masters of Sciences (MSc) thesis

Prepared

By

Abu KAMARA

Chairman: Prof. Dr. Sebahattin BEKTAŞ .....
Ondokuz Mayıs University

Member of Jury: Prof. Dr. Okan ÖZGÖNENEL .....
Ondokuz Mayıs University

Assistant Prof. Dr. Sedat DOĞAN .....
Ondokuz Mayıs University

...../...../.....

Prof. Dr. Hüseyin DEMİR

Institute Registrar

ACKNOWLEDGEMENT

There are many people who helped me in this work. First and foremost, I would like to thank my thesis advisor, Assistant. Prof. Dr. Sedat DOĞAN . Sedat guided me through this work, and with his constant expressions of "this shouldn't work", kept me on track. Sedat is smart, funny and easy going; excellent qualifications for any advisor.

I would like to express my respects and gratitude to Prof. Dr. Sebahattin BEKTAŞ, head of Department of Geomatics / surveying Engineering, Ondokuz Mayıs University Samsun - Turkey, for putting me on my feet to work more harder. His discussions were giving me the strength to reach for the stars and chase my dreams. Associate Prof. Dr. Yasemin ŞİŞMAN was my first supervisor, Lecturer at the Department of Geomatics / surveying Engineering, Ondokuz Mayıs University Samsun - Turkey. Her advices and discussions were provided to help me understand the basic concepts in Geomatics Engineering, and her directions and encouragements were really useful in this research. With all due respect, I wish to thank the following lecturers of the Department; Associate Prof. Dr. Faik Ahmet SESLİ, Assistant Prof. Dr. Aziz ŞİŞMAN and Assistant Prof. Dr. Derya ÖZTÜRK for teaching me the principles involved in this discipline of my career. May Allah bless you all.

Thank you, Allah, for always being there for me.

This thesis is only a beginning of my journey.

Finally, I would like to thank my adopted family. Fatma CESUR and son Murat CESUR have always been a source of constant support and encouragement. From them I have gotten a love of knowledge and the desire to work hard to achieve one's goals. I acknowledge my uncle Mr. Lawrence M. KAMARA and wife Mrs. Letticia KAMARA, aunt Omu ROGERS for their moral and financial supports. My regards to Mr. Alper Yiğitoğlu the General manager at Motif Harita for his assistance in collecting the data for this research. My last and final thanks go to all those whose names I didn't mention, you all in diverse ways made me the man I am today and I am forever grateful.

DEDICATION

This thesis is dedicated to the memory of my parents Mr. Abdulrrahman KAMARA, Mrs Lucia ROGERS and grandmother Massah KOROMA. I miss you all everyday, I love you all but Allah love's you most.

Also, this thesis is dedicated to my fiancé who has been a great source of motivation and inspiration.

Finally, this thesis is dedicated to all those who believe in the richness of learning.

TABLE OF CONTENTS

Pages

ACKNOWLEDGEMENT.....iv

DEDICATION.....v

TABLE OF CONTENTS vi

LIST OF TABLES.....viii

LIST OF DIAGRAMS.....ix

SIGNS AND ABBREVIATIONS.....xi

ÖZET.....xii

ABSTRACT.....xiii

1. GENERAL INTRODUCTION.....1

1.1 Introduction.....1

1.2 Aim of the Thesis and Methodology.....2

1.2.1 Aim 2

1.2.2 Methodolgy.....2

2. LİDAR TECHNOLOGY; A GENERAL SURVEY.....7

2.1 Physical Principle of LİDAR.....9

2.1.1 The Properties of Data sets, Obtained by LİDARS.....10

2.1.2 Secondary Plans and Procedures.....10

2.1.3 Preprocessed of Laser Data (Filtering) 11

2.1.4 Georeferencing.....12

2.2 Coordinate Frames / Systems Used For Local Georeferencing (Objective Coordinate Systems, Laser Scanner Systems etc).....14

2.2.1 Registration of Coordinate Frames and the Data sets.....14

2.2.2 Visualization of 3D Laser Data.....21

2.2.3 The Softwares / and or Free Lidaries.....22

3. SURFACE MATCHING 32

3.1 Transformation Selection.....36

3.1.1 Elaboration of Surface Representation And Similarity Criterion.....37

3.1.2 Matching Establishment.....39

4. SURFACE RECONSTRUCTION.....40

4.1 Implicit vs Explicit Surface Description.....41

4.1.1 Orientation Based on 2D Image Edges and 3D LİDAR Edges.....42

4.1.2 Orientation Based on 3D Model Edges and 3D LIDAR Edges.....42

4.1.3 Orientation With Surface Patches.....43

4.1.4 Alternative Solution With Range Images.....44

4.2 Surface Patches.....44

4.2.1 Normal and Curvature Estimation.....45

4.2.2 Boundaries.....49

4.2.3 Identifying Boundary and Edge Points.....49

4.2.4 Discontinuities.....52

4.3 Roughness.....52

5. CASE STUDY.....53

6. CONCLUSION.....65

7. REFERENCES.....68

8**. CURRICULUM VITAE.....73**

LIST OF TABLES

Pages

Table 1.1. Laser Scanners and Their Specifications.....……..6

LIST OF DIAGRAMS

Pages

Fig.1.1a. Front view of the implemented building…….....…….....…….3

Fig.1.1b. Front and side view of the implemented building.....….4

Fig. 2.1. Simple registration.....….....……16

Fig. 2.2. Scanner Administration.....….....……..23

Fig. 2.3. Menu Bar.....…….....…….23

Fig. 2.4. Quick view of the scan building.....……...24

Fig. 2.5. Planar view of the building.....……...25

Fig. 2.6. 3D view of the building …….....……..26

Fig. 2.7. Quick view of the upper part of implemented building....…….....…27

Fig. 2.8. Quick view of the upper part of implemented building.....….27

Fig. 2.9. Quick view of the upper part of implemented building.....……..28

Fig. 2.10. Planar view of the upper part of implemented building.....28

Fig. 2.11. 3D view of the upper part of implemented building.....29

Fig. 2.12. 3D view of the upper part of implemented building.....29

Fig. 2.13. 3D view of the upper part of implemented building.....30

Fig. 2.14. Quick view of the front view of implemented building.....30

Fig. 2.15. Planar view of the front part of implementated building.....31

Fig. 2.16. 3D view of the front part of implementated building.....31

Fig. 3.1. 3D model from the left side.....32

Fig. 3.2. 3D model from the right side.....33

Fig. 3.3. Reconstructed 3D model.....33

Fig. 3.4. With changes in scale, position, 3D viewpoint, and brightness.....34

Fig 3.5. With changes in scale and position.....35

Fig. 4.1. Estimating normal vector and curvature of vertex v.....46

Fig. 4.2. Neighborhood selection for point P.....48

Fig. 4.3. Interior angle between adjacent faces of a triangular mesh.....52

Fig. 5.1. 3D view of the implemented building.....54

Fig. 5.2. 3D view of the implemented building.....55

Fig. 5.3. 3D view of the implemented building.....56

Fig. 5.4. 3D view of the implemented building.....57

Fig. 5.5. 3D view of the implemented building.....58

Fig. 5.6. Finely aligned registered surfaces (007 and 008).....59

Fig. 5.7. scan points of 001 surface.....60

Fig. 5.8. scan points of 006 surface.....61

Fig. 5.9. scan points of 007 surface.....62

Fig. 5.10. scan points of 008 surface.....63

Fig. 5.11. scan points of 008 surface.....64

Fig. 5.12. coordinates of K1 (control point) in VRML file format.....64

Fig. 5.13. coordinates of K1 (control point) in IGS file format.....65

Fig. 5.14. coordinates of K1 (control point) in DXF file format.....66

SIGNS AND ABBREVIATIONS

LİDAR	Light Detection and Ranging
DEM	Digital Elevation Model
DSMs	Digital Surveying Models
L	LİDAR
3D	Three - Dimensional
2D	Two - Dimensional
ICP	Iterative Closest Point
GPS	Global Positioning System
TLSs	Terrestrial Laser Scanner
ITGs	Information Technologies Group
LS	Laser Scanner
LSD	Local Shape descriptor
DTM	Degital Terrain Model
INS	Instrumental Navigation System
POS	Position and Orientation System
DBM	Digital Building Model generation / Digital Base Model
IMU	Inertial Measurement Unit
LAS	A binary file format for data storage
GCP	Ground Control Point
UTM	Universal Transverse Mercator
ICP	Iterative Closest Point
CMOS	Semiconductor

LİDAR VE DİJİTAL STEREO GÖRÜNTÜLER KULLANILARAK 3 BOYUTLU NOKTA BULUTU VE KATI MODELLERİN OLUŞTURULMASI

ÖZET

Bu tezin hazırlanmasının başlıca nedeni LIDAR alanında çalışan araştırmacılara, eğitimcilere bir kılavuz sağlama ihtiyacını karşılamaktır. Yöntemimiz, LIDAR teknolojisine dayanan yersel LIDAR tarayıcı kullanmaktadır. Analizlerimiz sırasında, sayısallaştırma işlemlerinde FARO lazer tarayıcı ve veri işleme süreci içinde FARO Scene yazılımı tercih edilmiştir. LIDAR tarayıcı sayesinde nokta bulutları nesneden/nesnelerden kolaylıkla elde edilmektedir. Lazer tarama teknolojisi ile birlikte bu tezin ihtiyaç duyduğu 3 boyutlu nokta koordinatları kolay ve hızlı bir şekilde elde etmek mümkün olmuştur. Bu araştırma sırasında bir binanın lazer tarama verileri kullanılmıştır..

Bu tezle, çeşitli alanlarda lazer tarama verilerinin değerlendirilmesi üzerine kapsamlı bir bilginin verilmesi amaçlanmaktadır. Ayrıca, nokta bulutunun 3 boyutlu register edilmesi temel kavramlar, matematiksel modeller ve bununla birlikte bu registrasyon işlemlerini yerine getirebilmek için kullanılabilecek ücretsiz, açık kaynak kütüphaneler açıklanacaktır.

LIDAR teknolojisindeki ve veri işleme sürecindeki dikkate değer gelişmelere rağmen bu alan, nispeten daha yeni bir konudur ve yakın gelecekte daha büyük değişiklikler olacaktır. Bu tezle, topografik uygulamalar için LIDAR teknolojisi hakkında sağlam bir giriş kaynağı oluşturmak istenmektedir. Ayrıca, teknoloji gelişirken buna bağlı olarak gelişecek olan veri işleme süreçleri hakkında da kapsamlı bilgi sunulacaktır.

Anahtar Kelimeler: LIDAR; Sayısallaştırma; FARO scene; Registrasyon; Nokta Bulutu Verisi; Veri İşleme

3D RECONSTRUCTION OF POINT CLOUDS AND SOLID MODELS FROM LIDAR AND DIGITAL STEREO IMAGES

ABSTRACT

The primary objective of this thesis is to meet the need and present a manual to the LiDAR research, practice, and educate communities. Our method used was ground based LIDAR which is one instruments of LIDAR technology. In doing our analysis, the FARO laser scanner was used in the digitization processed and FARO scene software for data processing. By using LIDAR method, point clouds can be easily obtain from object(s) i.e, with LIDAR; laser scanning technology, it is possible to obtain 3D point coordinates very fast and with ease which was implemented in this thesis. The research was done on a building .

The thesis aims at giving a comprehensive information on evaluation of the laser scanner data for one or more varieties of fields.

On the other side, the thesis will explan the 3D registration of point clouds data; its underlying concepts, mathematics models as well as the free - open source libraries to be used to perform these registration tasks.

Despite the remarkable achievements in LiDAR technology and data processing, it is still a relatively young subject and would likely change its course rather quickly in the near future. We expect this thesis can serve as a durable introduction to the fundamentals, principles, basic problems, and issues in LiDAR technology for topographic applications. It also provides a rather comprehensive and sophisticated coverage on various data processing techniques, which we believe will sustain and ultimately lead to new developments while the technology is advancing.

Key Words: LIDAR; Digitizing; FARO scene; Registration; point clouds data; Topographic; Sophisticated

1. GENERAL INTRODUCTION

1.1 Introduction

LIDAR technology is probably the most significant technology introduced in mainstream topographic mapping in the last decade. The main advantage of the techinque is that it provides a direct method for 3D data collection. Furthermore, it is highly accurate because of the millimeter - and cetimeter - level laser ranging accuracy and precise sensor platform orientation supported by an integrated position and orientation systems (POS) when required (Topographic Laser Ranging and Scanning; Principles and processing; Edited by: Slan and Toth). Unlike the traditional photogrammetric methods, LIDAR directly collects an accurately georeferenced set of dense point clouds, which can be almost directly used in basic applications. However, the full exploitation of LIDAR's potentials and capabilities are challenges for new data processing methods that are fundamentally different from the one used in basic applications. Over the last decade, there have been many significant developments in this field, mainly resulting from multidisciplinary research, including computer version, computer graphics, electrical engineering, and photogrammetry.

Although there have been many studies and applications since introduction of LIDAR, a conprehensive compilation is still missing. The main purpose of this thesis is to present a manual to the LIDAR users / applications as well as describing the problem of registration and fusion tasks of the LIDAR data.

The overall LIDAR data evaluation process will be explained with its main tricks and models within a real application. The thesis will also discuss the open - source libraries to be used for LIDAR data processing.

In the next chapter, we'll give the aims of the thesis and the methodology to be followed to provide those aims. In section 2, we'll give the general physical and mathematical stages; from acquision of data, preprocessing operations, registration tasks, fusion of LIDAR data with other data sets, and finally manual, semi - automatic and / or automatic procedures used for interacting laser data such as

editing, measuring, higher level feature extracting etc. All of these concepts will be applied in a real project and this application will be given explicitly in section 3 with its main tricks and necessary details.

1.2 Aim Of The Thesis And Methodology

1.2.1 Aim

The main purpose of this thesis is to present a manual to the LIDAR users / applications as well as describing the problem of registration and fusion tasks of the LIDAR data. In this thesis, we will be discussing the advantages and disadvantages of the most prominent method; digital stereo images. There will be an emphasizes on the need for explicit surface descriptions. Combining the advantages of LIDAR and stereo image photogrammetry is an interesting fusion problem.

1.2.2 Methodology

There are four (4) instruments of LIDAR technology. These are;

1. Profiling LIDAR
2. Small- footprint LIDAR
3. Large-footprint LIDAR and
4. Ground Based LIDAR

In this thesis, the method used is Ground - Based LIDAR. A case study is on a governmental building which has now been privatized. The private owner wishes to change this building into a hotel. The building is located at Gayrettepe in İstanbul / TURKEY. İstanbul is divided into two sections which includes Europe and Asia. Gayrettepe is on the European side of İstanbul. See photographs of implementation building below in figure 1.1a and 1.1b



Fig.1.1a. Front view of the implemented building



Fig.1.1b. Front and side view of the implemented building

Ground Based LIDAR method was implemented, measuring starts by first illustrating the control points on the surface. Control points can be either a white round ball or a number written on A4 / A3 paper. The control points illustration must be in a 3D form as the scanner rotates at $360^{0.}$ FARO laser scanner was used and placed in thirty-eight (38) suitable positions to do the recordings. At each position recording was done for nine (9) minutes, but this can be extended up to thirty (30) minutes or more upon demands. The data was then inputted in a software called

FARO scene for processing. Filteration was done to helped verified control points on surfaces. Removing unwanted points is a central and an unavoidable process in preparing point cloud data for building model reconstruction, be it automatic or manual. This owes to the fact that, laser scanners lack the ability to selectively scan only the objects of interest. The resulting point cloud obtained from a laser scanner is thus a composition of points from objects within its field of view and focal range. Proper filtering can help in the elaboration of control points. That is, depending on the scanner position (distance) from the control point it can be well seen or not. If the pulse hits the surface and returns back like an alpha particle, it can result in a good pixel of that surface, but if on the other hand it hits and passes through the surface then there can be a parallax for that surface, which means that the number on that surface cannot be seen well. Control points or scans which are not well seen must be eliminated in other to get a better accuracy. The accuracy for the implementation work in this thesis was 5mm. Filtering can sometimes be done by automatic means in the FARO scene or done manually (that is, giving the control points numbers you wish one by one but non of the number will be repeated).Whilst using the software, you can give the control points a number you wish. Therefore, if accuracy is not to be compromised for automation, removal of irrelevant points is better done manually. Manual removal of irrelevant points, as done in this thesis, basically entails visually identifying such points, manually selecting and deleting them. Because a terrestrial scanner is usually stationed at different locations in order to obtain a complete scan of a building, this process is done on every individual scan to obtain roughly cleanse data before registration. In this thesis manual labelling of control points was done. In table 1.1 there are list of few scanners including implemented scanner (FARO scanner) with their accuracies.

Table 1.1. Laser Scanners and Their Specifications

Firm	Type	Measurement Range (m)	Meas. Point	Scanning Angle	Distance Accuracy	Position Accuracy	Light Beam
Leica	Scan Station	300m (90% Reflection)	4000 point/sec.	270°(V) 360°(H)	4 mm @ 50 m	6 mm @ 50 m	4 mm @ 50 m
	HDS3000	300m (90% Reflection)	4000 point/sec.	270°(V) 360°(H)	4 mm @ 50 m	6 mm @ 50 m	4 mm @ 50 m
	HDS4500	53.5 m	500000 point/sec.	310°(V) 360°(H)	5 mm+120pp m (%100yns.y.)	13.7 mm @ 25 m	8.5 mm @ 25 m
	HDS6000	79m (80% Reflection)	500000 point/sec.	310°(V) 360°(H)	5 mm @ 50 m	10 mm @ 50 m	3 mm+ 0.22mrad
Optech	Iıris 3D	3m-1500m (80% Reflection)	2500 point/sec.	310°(V) 360°(H)	7 mm @ 100 m	8 mm @ 100 m	0.00974°
Riegl	LMS-Z420	2m-1000m (80% Reflection)	12000 point/sec.	0-80°(V) 0-360°(H)	8 mm @ 50 m	10 mm @ 50 m	0.25 mrad
	LMS-Z390	1m-300m (80% Reflection)	11000 point/sec.	0-80°(V) 0-360°(H)	4 mm @ 50 m	6 mm @ 50 m	0.25 mrad
	LMS-Z210	4m-650m (80% Reflection)	12000 point/sec.	0-80°(V) 0-360°(H)	10 mm @ 50 m	15 mm @ 50 m	2.7 mrad
Z - F	Imager 5006	1 m - 79 m	500000 point/sec.	310°(V) 360°(H)	mm @ 50 m	1 mm @ 50 m	0.22 mrad
Faro	LS 880	1 m - 80 m	12000 point/sec.	320°(V) 360°(H)	3 mm	5 mm	0.01°

2. LIDAR TECHNOLOGY; A GENERAL SURVEY

LiDAR has emerged as an important source of data for the generation of 3D city models. The main advantage is the direct acquisition of a reliable and dense 3D point cloud in contrast to the error-prone matching techniques when using stereo or multiple images. The LiDAR research community has been very active in the development of algorithms for the post-processing of LiDAR data, especially for DBM generation (Alharthy, 2003; Charaniya, 2005; Maas and Vosselman, 1999; and Vosselman, 1999).

A classification procedure to separate terrain and off-terrain points is usually performed to help with the building detection. A substantial portion of existing techniques is based on mathematical morphology and includes the methods presented by Kilian et al. (1996), Vosselman (2000), Roggero (2001), and Zhang et al. (2003). In the proposed method by Vosselman (2000), the classification of LiDAR data is based on two operations: morphological erosion using a pre-defined discriminant function and comparison between the eroded and original surfaces. A point is classified as a terrain point if its original height does not exceed the height of the eroded surface at the same location. A variation of this method was proposed by Roggero (2001), where the terrain is extracted using a local morphological operator. The shape of this operator is designed according to the slope of the bare earth. Since the shape of the bare earth is not known, a local linear regression procedure is used to derive an estimate of its shape.

The off-terrain points usually include points that belong to trees and buildings. By using attributes, such as surface roughness, buildings can be distinguished from trees. In the reconstruction process, planar roof patches are segmented in the detected building regions. Segmentation techniques can be roughly divied into two categories (Vosselman, 2004). The first category includes the techniques that segment point clouds based on the proximity of points and the similarity of the locally estimated attributes from the surface. The techniques belonging to the second category aggregate points with similar attributes into clusters in a parameter space (or attribute space).

Several researchers (Hoover et al., 1996; and Lee and Schenk, 2001) utilized the region growing method proposed by Besl and Jain (1998), which extends seed regions to adjacent points while considering the proximity and attribute similarity of points for segmenting LiDAR points. In comparison to the region growing method built in the spatial domain, there are some techniques which segment points in the parameter space (or attribute space). Vosselman and Dijkman (2001) extended Hough transform (Hough, 1962) to deal with planar surfaces in 3D. Instead of focusing on extracting planar surfaces, some researcher developed clustering methods offering generality and flexibility in accomodating spatial relation and attributes to distingush different types of surfaces such as vegitation, smooth surfaces, and planar surfaces (Axelsson, 1999; Mass, 1999; Filin, 2002; Vosselman et al., 2004; and Filin and Pfeifer, 2006). These methods are based on an attribute vector (which consistes of the proximity of points, the parameters of the tangent plane, and relative height different between the points) defined by a point and its neighbouring points (Axelsson, 1999; Mass, 1999; Filin, 2002; Vosselman et al., 2004; and Filin and Pfeifer, 2006).

After the planar patches are acquired from the segmentation process, building boundaries can then be modeled. Intersection of surface patches and regularization of the patch boundaries are utilized by Vosselman (1999), Mass and Vosselman (1999), and Sampath and Shan (2007). The problem associated with building reconstruction using only LIDAR is that building outlines are not determined precisely. This can be explained by the irregular and sparse nature of the LIDAR data. In other words, there is no guarantee that the LIDAR footprints will capture surface discontinuities such as building boundaries. Hence, the accuracy of the generated building boundaries will be highly dependent on the LIDAR point density (Wang et al., 2008).

Lidar has become an established method for collecting very dense and accurate elevation data across landscapes, shallow-water areas, and project sites. This active remote sensing technique is similar to radar but uses laser light pulses instead of radio waves. Lidar is typically “flown” or collected from planes where it can rapidly collect points over large areas. Lidar is also collected from ground-based stationary (Figure 1.1a and 1.1b) and mobile platforms. These collection techniques are popular within the surveying and engineering communities because they are capable of producing extremely high accuracies and point densities, thus permitting the

development of precise, realistic, three-dimensional representations of railroads, roadways, bridges, buildings, breakwaters, and other shoreline structures.

Collection of elevation data using lidar has several advantages over the most other techniques. Chief among them are higher resolutions, centimeter accuracies, and ground detection in forested terrain.

The three-dimensional coordinates (e.g., x,y,z or latitude, longitude, and elevation) of the target objects are computed from 1) the time difference between the laser pulse being emitted and returned, 2) the angle at which the pulse was "fired," and 3) the absolute location of the sensor on or above the surface of the Earth.

Lidar systems are active systems because they emit pulses of light (i.e. the laser beams) and detect the reflected light. This characteristic allows lidar data to be collected at night when the air is usually clearer and the sky contains less air traffic than in the daytime. In fact, most lidar data are collected at night. Unlike radar, lidar cannot penetrate clouds, rain, or dense haze and must be flown during fair weather.

Many lidar systems operate in the near - infrared region of the electromagnetic spectrum, although some sensors also operate in the green band to penetrate water and detect bottom features.

A rule of thumb is that if you can look up and see the sky through the trees, then that location can be measured with lidar. For this reason, collecting lidar in "leaf off" conditions is advantageous for measuring ground features in heavily forested areas (Jamie Carter, Keil Schmid, Kirk Waters, Lindy Betzhold, Brian Hadley, Rebecca Mataosky, and Jennifer Halleran; November, 2012).

2.1 Physical Principles of LIDAR

Both pulsed and continuous wave lasers are being used. Pulsed systems measure the round-trip time of a short light pulse from the laser to the target and back to the receiver. Continuous wave systems carry out ranging by measuring the phase difference between the transmitted and received signal. This state-of-the-art focuses on pulsed systems.

3D point cloud is obtained by direct georeferencing processes: a system using both GPS (differential measurements with a ground station located near the survey area) and inertial measurements (IMU) is used to optimally calculate supporting vector attitudes and the absolute orientation of the laser sensor (Heipke et al., 2002).

Basic lidar systems consist of a laser transmitter and a receiver (rangefinder unit which receives the reflected pulses and measures the distance), a mechanical scanner, a hybrid positioning system, a storage media, and an operating system for signal digitization and on-line data acquisition. This unit monitors and synchronizes measurements, and processes data in real-time to extract georeferenced points (Baltsavias, 1999a; Thiel and Wehr, 2004).

2.1.1 The Properties of Datasets, Obtained by LIDARS

Very early lidar systems actually recorded only one discrete, either the first peak or the final peak in the reflected wave. By 2000, commercial systems become capable of measuring multiple (3 - 5) returns per pulse. These multiple returns can be analyzed and classified to produce information about objects above the surface.

The more returns that are recorded the larger the resulting dataset becomes. Lidar datasets tend to be very large, due simply to the high emitted pulse rates. Add to that, multiple returns per emitted pulse, and the size of the dataset grows geometrically. Early multiple return systems were designed to record up to 5 return pulse, but analysis of datasets showed that, in practice, 4th and 5th returns almost never occured. Most lidar systems designed today for topographic mapping are optimized to record 3 return pulses. First returns can be used to create digital surface models that include features above the ground surface, such as buildings, bridges, and trees canopy. Intermediate returns are helpful in separating vegetation from solid objects among the ground features. Final returns are approximation of the bare ground surface (Jensen, J.R. 2007).

Lidar data, stored as either LAS file, LAS datasets, or terrains, can be added to a mosaic datasets directly, without converting them to a raster before adding them. The output of a mosaic dataset will be a raster.

Lidar data can be managed within a mosaic dataset by adding the LAS datasets, or terrain dataset. For example, you can add all your LAS files, from all your diferent acquisitions, and use the mosaic dataset as the single source for finding the data as it's needed.

Using the mosaic dataset, you can also serve the Lidar data as an image service providing access to the intepolated surface, or even to allow user to download the source files.

A LAS dataset to be used to edit the classification used by the LAS files. If the LAS files are modified, they will be updated in the mosaic dataset directly .

2.1.2 Scanning Plans and Procedure

Before the scanning commences, the project area shall be reconnoitered to determine the best time to collect data to minimize excessive “artifacts” from traffic or other factors, and to identify obstructions that may cause data voids or shadows. Check weather forecast for fog, rain, snow, smoke, or blowing dust. Tall tripod set-ups may be used to help reduce artifacts and obstructions from traffic and pedestrians. Areas in the project that will be difficult to scan should be identified and a plan developed to minimize the effect on the final data, through additional set-ups or alternate methods of data collection. Safety should always be taken into consideration when selecting setup locations.

Site conditions should be considered to determine expected scanning distance limitations and required scan density to adequately model the subject area.

The scanning starts by first applying control points on the object or image to be scan. The reason for such an approach is to collects 3D data that can be use in the analysis. One disadvantage of the laser scanner is that it scans lots of unwanted points. With the help of control points, coordinates from the scan image / object, can easily be obtain.

2.1.3 Preprocessed of Laser Data (Filtering)

Laser scanners have been increasingly used in recent years for the collection of terrain elevation data. The technology demands new processing technologies which have reached a stage of good practical application so far for the interpolatin of ground DTMs. Beyond pure ground DTMs, however, laser scanner data have great potential for other applications such as creation of digital building models or vegetation analysis. This thesis presents the state of the art of interpolation techniques along with a new technique to separate filtered data from non filter data even in a special case of off - terrain objects (building, trees) which would normally be eliminated from the ground model.

For the processing of laser scanner data a special algorithm has been developed and implemented in the DTM program package SCOP (N. Pfeifer, K. Kraus, A. Köstli, 1999). This algorithm estimates the skewness of the error distribution of the

laser scanner data buildings and assigns small weights to those points that show large positive errors during the results in a classification of the laser points in terrain and off - terrain (mainly building) points.

The data acquisition itself consists of several steps. The area of interest will be scanned in one or more scenes. The immediate result is a point cloud, in which each point is represented by 3D-coordinates (x, y, z) and the intensity of the reflected signal (i). The fusion of several point clouds in one (global) coordinate system (often called “registration”) is realized either with pass points or with natural structures in the point clouds. The method with pass points is the most precise one. The use of a tacheometer in conjunction with pass points offers several advantage (Marrakech and Morocco, 2003):

- no overlapping areas in the scans are necessary
- the scan is geometrically controlled
- a transformation into a geodetic coordinate system or into a local, gravity related system is possible.

2.1.4 Georeferencing

Georeferencing is the process of assingning spatial coordinates to data that is spatial in nature, but has no explicit geographic coordinate system. In this thesis we displayed control points on the surface of a building (balls and numbers written on papers) and assign spatial coordinates to the image so that it can be overlaid with modern data.

As starting point to discuss georeferencing, we need to distinguish between the physical earth, the geoid, and a reference ellipsoid. The physical earth is what we try to measure and model (building), like in this thesis. The geoid represents a surface of constant gravity, which is idealized by the notion of mean sea level, but does not correspond to the actual level of the sea at any given point at any instant in time. A reference ellipsoid is a mathematically - defined shape that is a "best - fit" to the geoid, most often for a continent, but potentially for the entire globe. The challenge of geodesy, and charting is to develop well - defined, quantifiable relationships between the ellipsoid, the geoid, and the physical earth. This is particularly important when measuring the height of things, as we usually expect height to tell us two things: 1) the physical measurable distance between two objects in a "vertical" direction and 2) the difference in the gravitational potential energy between objects.

You should be realizing by now that these are not exactly the same thing. Furthermore, measuring the relative heights of two objects is a fundamentally different problem than establishing the elevation of a single point, because the term "elevation" implies that we know absolutely starting point (zero) is. This may seem like an incredibly trivial point, but by the end of this thesis, you will hopefully see and able to explain why it isn't quite so simple.

There are two fundamental methods of referencing spatial data:

The first – known as the geo-centric system – uses a 3-D coordinate system with the centre of the earth acting as the origin of the three axes. This method is universally used in scientific applications, but it is user unfriendly when applied to points on the earth's surface. This is because the axes are made parallel to the spin axes of the earth rather than north (or some other arbitrary direction). The system can be expressed in two ways: either as a 3-D Cartesian coordinate of the form x,y,z; or as longitude (λ), latitude (φ) and height (H) above a known reference surface – the ellipsoid. It is important to note that the x and y do NOT refer to east and west or north and south.

The second, more common, system is the projection. This takes the 3-D coordinates and expresses them as a plane plus height above it. In other words, it flattens out the curved earth in a small region to a flat surface. Coordinates on the plane tell us where a particular point within the projection is being used and are measured as distances, east and north from the starting point or origin.

To avoid errors, the extent of the projection is usually limited to a small part of the earth's surface. Choice of projection is dependent on the area of the world being considered.

Different projections have different properties. Spatial data users choose the projection that provides the least distortion – in distance, direction, scale, area and so on – within the region being considered.

Bear in mind that there are dozens of different types of projection and each can have hundreds of different definitions depending on where they are used. In Great Britain the chosen projection is known as the National Grid.

Once the digital data has been georeferenced, you can display the information in an infinite number of ways.

In one way, georeferencing can be considered as registration to a global frame, since the operation involves coordinate transformation in the same way as

registration. The difference is while registration involves at least two scans, georeferencing can be applied to one scan. Two methods of georeferencing are available (Yezeed Abdelmajid, 2012):

1) Direct georeferencing;

Here for each scan, the local coordinate system is transformed directly to the global system by using coordinate transformations. This can be achieved through two methods:

- By using ground control points (GCP) to compute the global coordinates of some scanned targets, and then the rigid body transformation can be used.
- By using the scanner to directly georeferencing the scanned point. This option requires the scanner to be equipped with optical plummet and a level bubble, allowing centring over a known point and levelling (Scaioni 2005). The coordinate of the scanner can also be obtained using total station or a mounted GPS (Reshetyuk 2009).

2) Indirect georeferencing;

Here all scans are to be registered to one scan by using common targets/features; and thereafter transforming this final scan coordinates to the global system using ground control points. Such as registration, indirect georeferencing require a certain amount of overlapping. In laser scanning software, the georeferencing involves the transformation of coordinates between two systems, and is regarded as a rigid body transforming achieved through closed forms.

2.2 Coordinate Frames / Systems used for Local Georeferencing (object, coordinate system, laser scanner systems etc)

It is clear that points and features on, above and below the earth's surface have position. To express that position, you need to choose an appropriate coordinate system so that positions can be defined within it. Such a system must obviously give each point a different coordinate.

There are thousands of coordinate systems in use throughout the world. It is possible for a user to invent their own and, indeed, this is often done for large engineering works. The disadvantage is that points outside the area of the bespoke (building) system cannot be coordinated within it and the relationship between the bespoke (building) and other systems is hard to define.

Many national mapping agencies have defined local referencing systems to meet their needs. In Britain, for example, they have the National Grid. These are perfectly acceptable when working within a country, but problems exist in drawing up multinational data unless there is cross-border convergence. In Europe local coordinate projections are often referred to the European Terrestrial Reference System 1989 (EtrS89) because it is fixed at a point in time and well defined.

Probably the most common global coordinate system in use today is the GPS-based World Geodetic System 1984 (WGS84). This is fixed to points on the earth's surface which move over time because of changes in the earth's crust. A significant global projection system is Universal Transverse Mercator (UTM). This is a defined set of projections that cover the whole world and allow countries to share spatial data more easily. The coordinate system used in this thesis for our implemented work is the local coordinate system.

2.2.1 Registration of Coordinate Frames and the Data Sets

Registration is a pre-processing step required if multiple scans are taken to capture a scene. It aligns and combines multiple data sets into one complete 3D cloud. Several approaches have been developed to address the registration task. One of the most popular algorithms is the Iterative Closest Point (ICP) algorithm (Besl and McKay, 1992) which requires an initial rough alignment between two clouds and then iteratively searches for point matches to solve for a transformation. Other methods utilize targets (Yu, Ferencz, and Malik, 2001) or feature points (Gelfand et al., 2005; Barnea and Filin, 2008) to determine the required transformations. However, registration is now a tool that is commonly available in laser manufacturer software programs, and hence, it was not a focus of this thesis alone. Consider a simple concept of registration below;

Combine small overlapping images into single large image.

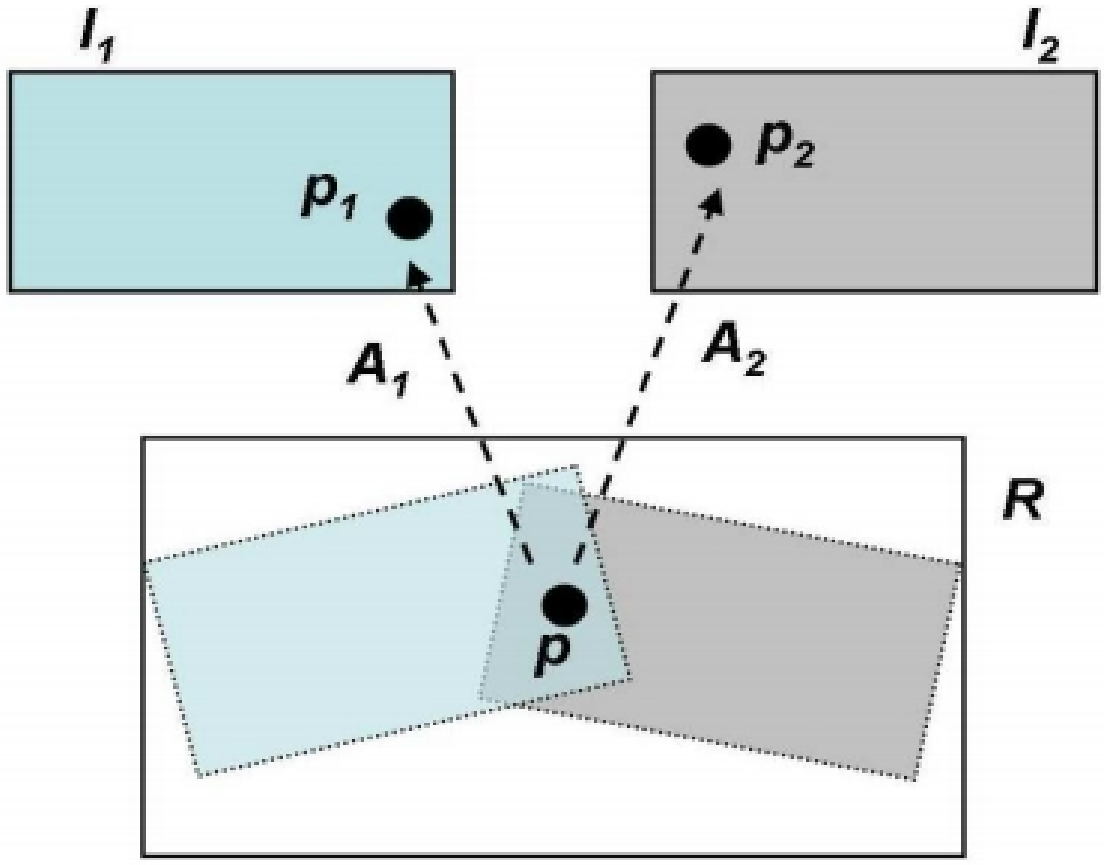


Fig. 2.1. Simple registration

From Fig. 2.1. above;

Suppose that $\mathbf{A_1}$ and $\mathbf{A_2}$ are known.

They specify the transformation between the output image **R** and the input images $\mathbf{I_1}$ and $\mathbf{I_2}$, respectively.

For eah pixel p in **R**, do:

- compute: $\mathbf{p_1} = \mathbf{A_1}\,\mathbf{p}$ and $\mathbf{p_2} = \mathbf{A_2}\,\mathbf{p}$.
- If both $\mathbf{p_1}$ and $\mathbf{p_2}$ fall outside of I_1 and I_2, respectively, then R(**p**) = default color, example black.
- If both $\mathbf{p_1}$ and $\mathbf{p_2}$ fall inside of I_1 and I_2, respectively, then R(**p**) = blending of $I_1(\mathbf{p_1})$ and $I_2(\mathbf{p_2})$.
- Otherwise, only one of $\mathbf{p_1}$ or $\mathbf{p_2}$ falls inside I_1 or I_2 .

So, $R(\mathbf{p}) = \mathbf{I_1}(\mathbf{p_1})$ or $\mathbf{I_2}(\mathbf{p_2})$, as appropriate.

Most objects are big enough to be scanned from one position, as obstacles may prevent scanning of some sides, and so there is always a need to do different scans form distinct positions or viewpoints in scanning projects. This will lead to a number of different scans of the object with different coordinate systems, and these different

scans are needed to set together in one scan with a common coordinate system for the whole object.

The process of setting a common scan of an object from scans with different coordinate systems is known as registration or aligning.

Registration is the process that involves the alignment of two or more point data sets in different coordinate systems to each other, resulting into one coordinate system for both.

In the laser scanning systems, the process is achieved by transforming the coordinate system of one of the point sets to the other point set coordinate system by applying specific translations and rotations in means of rigid body transformations (six degrees of freedom), where the shape and size are preserved (Scale factor is unity – orthogonal transformation).

Thus, in principle, registration is considered as coordinate transformation problem that involves translations and rotations, and the problem is a sub group of the general affine coordinate transformation, solved in the manner of similarity or rigid body transformation.

This coordinates transformation problem can be represented as a least square problem which is solved by minimizing the square of error as in equation (2.2) (Yezeed Abdelmajid, 2012).

$$\boldsymbol{A_i = RB_i + T} \tag{2.1}$$

$$\varepsilon^2 = \sum_{\mathbf{i}=1}^{\mathbf{n}} \left\| \mathbf{A_i} - \left(\mathbf{RB_i} + \mathbf{T} \right) \right\|^2 \tag{2.2}$$

where **A**, **B** are coordinates of point sets in two different coordinate systems, **R a**nd **T** are rotation matrix and translation vector, respectively.

In the Cartesian coordinate system, rotation in rigid body transformation is normally represented through two ways:

Euler's angle rotation representation;

Euler angels are rotation angles that applied to each axis to form the desired rotation successively. By applying these angles on the coordinate system rotation axes X, Y and Z successively, the rotation matrix **R** in (2.3) is parameterized by:

$$R=\begin{bmatrix} \cos r_y \cos r_z & \cos r_y \sin r_z & -\sin r_y \\ -\sin r_x \sin r_y \cos r_z + \cos r_x \sin r_z & \sin r_x \sin r_y \sin r_z + \cos r_z \cos r_x & -\sin r_x \cos r_y \\ \cos r_x \sin r_y \cos r_z + \sin r_x \sin r_z & -\cos r_x \sin r_y \cos r_z + \sin r_x \cos r_z & \cos r_x \cos r_y \end{bmatrix} \quad (2.3)$$

where r_x, r_y, r_z are the rotation angles about x, y, z axes, respectively.

Axis and angle rotation representation;

Euler angles could suffer from gimbal lock problems when used for rotation representation; an alternative way is to represent the rotation by defining a rotation angle around an arbitrary axis. This can be achieved by using quaternion.

To represent a rotation by angel (θ) around vector [e_1 e_2 e_3], the rotation matrix **R** in (2.3) is parameterized by using the unit quaternion [q_0, q_1, q_2, q_3]:

$$R_q=\begin{bmatrix} q_0^2+q_1^2-q_2^2-q_3^2 & 2(q_1q_2-q_0q_3) & 2(q_1q_3-q_0q_2) \\ 2(q_1q_2-q_0q_3) & q_0^2+q_1^2-q_2^2-q_3^2 & 2(q_2q_3-q_0q_1) \\ 2(q_1q_3-q_0q_2) & 2(q_2q_3-q_0q_1) & q_0^2+q_1^2-q_2^2-q_3^2 \end{bmatrix} \quad (2.4)$$

$$q_0=e_1\sin\left(\frac{\theta}{2}\right),\ q_1=e_2\sin\left(\frac{\theta}{2}\right),\ q_2=e_3\sin\left(\frac{\theta}{2}\right)\ \&\ q_3=e_1\sin\left(\frac{\theta}{2}\right) \quad (2.5)$$

The translation **T** is parameterized by the translation vector

$$[t_1\ \ t_2\ \ t_3] \quad (2.6)$$

Different approaches are used for the computations of the transformation parameter; they vary between iterative and closed-form solutions. These approaches mainly differ in the representation of rotation and translation, and the used error minimizing criteria (Eggert et al., 1997).

Mostly, the closed-form solutions are preferred due to their stability. Different closed-form solutions are proposed; mostly used methods are singular value decomposition (SVD) (Arun et al. 1987), orthogonal rotation matrix by (Horn et al., 1988) and quaternion methods (Faugeras and Hebert, 1986) (Horn, 1987) and (Akca, 2007).

In SVD method, the fact that the two point sets have similar centroids used. A correlation matrix is computed between the two point sets using their centroids. The rotation matrix is obtained by getting the singular value decomposition of this matrix, and the obtained rotation matrix is used to compute the translations (Arun et al. 1987), (Umeyama, 1991) and (Kanatani, 1994).

Orthogonal matrix method is used by (Horn et al., 1988) in a method similar to SVD in using the centroid to compute a correlation matrix. The rotation matrix is computed by using the eigenvalue and eigenvectors (Eggert et al., 1997) (Horn et al., 1988).

Closed form solutions are generally superior to iterative methods, in terms of efficiency and robustness, because the latter suffer from problems of not guaranteeing convergence, becoming trapped in local minima of the error function and requiring a good starting estimate (Eggert et al., 1997). Thus, the closed forms are preferred to calculate the transformations in the laser scanning software.

In terrestrial laser scanning software, there are two general methods used for registration; registration using target and registration using features (cloud registration), both methods depends on the above rotation and translation computations. Our target or feature in this thesis is on a building (Fig. 1.1a and Fig. 1.1b) , by using point clouds a 3D model reconstructed .

Registration using targets;

In this method, identical points with known coordinates in the different point sets are used as registration targets to find the transformations parameters (Fig.2.1). The computation uses anyone of the above mentioned methods, but mainly the closed forms are used.

In general, any part of the scanned point cloud with known coordinates can be used, providing that it is available and easy to recognize in both scans.

The matching of targets for the registration purpose can be described by one of the following conditions:

- Coincident matching
- Coplanar matching
- Collinear matching

The first condition can be applied to all types of targets, where the latter are only used with modelled or extracted features of the point cloud, and require some variation in axes directions.

It is important for the registration algorithm to be able to identify and distinguish between these registration targets. Some of them can use the target identity key (label) to match the identical targets while in some others; there is a

need to specify these targets prior to the scanning process. It is also possible in most software to specify targets by manual on screen picking.

Some softwares allow for analysing the quality of targets by measuring statistics about them prior to registration process.

Once the targets are specified, the transformation parameters are computed and applied to the other point set.

Registration using cloud features;

Other method for registration in laser scanning software is by using cloud features. The method is also known as the cloud-to-cloud registration, where the features of point cloud are used to compute the transformation parameters. By cloud features in this thesis, we mean the point and shape features of scanned point clouds (different surfaces), mainly the topological information of the building and the geometry of the scanned points. This includes points, lines and surfaces. Some of these methods use the intensity/colour information beside the geometrical information. This features information is used to identify and calculate relationship between two point clouds sets, which is used to compute the alignment between the two sets by minimizing the sum of squared errors between these corresponding features.

In feature based methods, points or surface shapes are used as features, where their correspondence in the other point set are searched and the distance between the points and their correspondence is minimized with the least square resulting into the transformation parameters. The most known feature based method is the iterative closest point (ICP) developed by Besl and McKay (1992), Chen and Medioni (1992) and Zhang (1994), which matches each point in one cloud set to its closest point in the other set, and the rigid body transformation is obtained by minimizing the distance between the sets. This procedure is iterated until a convergence is achieved (Akca, 2007).

Surface matching methods are also known, where two surfaces are matched to each other and distance between them is minimized with the least square criterion. The surface matching methods are based on the iterative closest point (Reshetyuk, 2006).

Iterative closest point;

The iterative corresponding point or better known as the iterative closest point is an effective method used for registration point clouds.

In general, iterative closest point algorithm involves the following steps:

- Selecting of points.
- Finding and matching points to their corresponding ones.
- Minimizing the distance arriving into the transformations.
- Iterate the solution based on the computed values.

Mainly, the iterative closest point requires two conditions:

- Sufficient overlap with variant features between the point sets.
- Initial alignment between the points to run, which is normally achieved through tie points or common features.

The transformation parameters in the iterative closest point are usually computed by using one of the above-mentioned closed forms solutions (Akca, 2007). There are two factors affecting the efficiency of the iterative closest point (Besl and McKay, 1992):

- There should be a valuable variation in the point cloud geometrical shape for the sets.
- There should be sufficient overlap between the two sets.

Many variants of the iterative closest point are developed since its introduction concerning its robustness and speed. These developments mainly affect the algorithm in one or more of its above - mentioned stages. Some developments are on the selection of points used by the algorithm or their matching criteria while others on error minimizing criteria and transformation calculations (Rusinkiewicz and Levoy 2001). The iterative closest point can be used with different types of geometrical representations, including points, lines, and surfaces. Usually, a combination of the target based and feature based methods is used to achieve the best registration results in laser scanning software.

In laser scanning software, the use of iterative closest point is always accompanied with tools to achieve the pre-alignment step. This is done either manually through mouse orientation or by using target points. Another method for registration in laser scanning is by using modelled features, which are directly modelled or extracted from the point cloud. Depending on the type of the modelled feature, the registration can be carried out either through target registration method or the iterative closest point principle. A method of registration based on the same idea

of iterative closest point is to use extracted features as corresponding features. This may overcome the necessity for initial orientation and reduce the searching stage to a small number of features (Oztireli and Basdogan, 2008).

2.2.2 Visualization of 3D Laser Data

In laser scanning software, 3D modelling is the process of obtaining a digital mathematical representation of an object in three dimensions. This representation is used in the computer environment for the visualization, measuring, manipulating, documentation and processing purposes, in a way that satisfies the engineering need.

Three-dimensional modelling is known in some literature as geometric modelling, and has its roots back into the 1960s and 1970s. A lot of developments from different fields of applications contribute to 3D modelling such as engineering and product design, computer-aided manufacturing, electronic and medical prototype, computer vision, computer graphics as well as robotic and motion planning (Hoffmann, 1989).

The treated data is visualized in different ways:

- Point clouds in a 3D-projection, with color or greyscale-coded intensity representation, is often used as a first visual check of the acquired data.
- Point clouds can also be combined with derived geometrical elements.
- "True" Ortho-Photos are realized by the fusion of digital images (point information) and the registered point clouds (geometry).
- 3D-Models
- "Virtual flights" through the modeled scene.

2.2.3 The Softwares / and or Free Libraries

The softwares / free libraries used in this thesis for data analysis are; FARO scene, Matlab, cloudcompare, and many more . FARO scene were used for more detail analysis in this thesis (quick view, planar view and 3D view) whilst Matlab, Cloudcompare and the other free libraries were used for analysis of cloud points.

SCENE is a comprehensive 3D point cloud processing and managing software tool for the professional user. It is specially designed for the viewing, administration, and working with extensive 3D scan data obtained from high resolution 3D laser scanners like the FARO Focus^{3D}. SCENE processes and manages scanned data both highly efficiently and easily by offering a wide range of functions and tools, like

filtering, automatic object recognition, scan registration and positioning as well as automatic scan colorization. Once SCENE has prepared the scan data, you can commence evaluation and further processing right away. For this, it offers functions from simple measuring to 3D visualization through to meshing and exporting your scan data into various point cloud and CAD formats.

The built-in FARO Focus^{3D} scanner administration functionality of SCENE allows you to manage your Focus^{3D} SD cards, scanner snapshots and your scan projects.

You can open the scanner administration of SCENE under View > Administration View or in the projects selector by clicking on the Scanner Administration button.



Fig. 2.2. Scanner Administration.

Where; 1 - Structure View and

2 - Administration View.

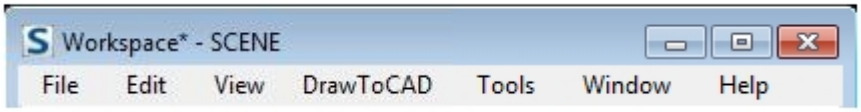


Fig. 2.3. Menu Bar.

There are various views to display and explore scans and point clouds using FARO scene software:

Quick View;

The standard scan view to examine single scans. For this, the scan does not have to be loaded. The quick view is available within a few seconds; in the meanwhile the scan data will be loaded in the background. You can manipulate the scan points as soon as background loading is finished. Until then you are only able to view and navigate.

Planar View**;**

Used to examine single scans. The scan must be loaded; this will happen automatically if required.

3D View;

The 3D view is not limited to display the scan points of a single scan or scan point cloud, it also offers the combined viewing of all the scans and objects in your project point cloud or workspace.

Figure 2.4. of this thesis shows the starting point of the scanned implemented building, quick view of the scan using FARO scene .

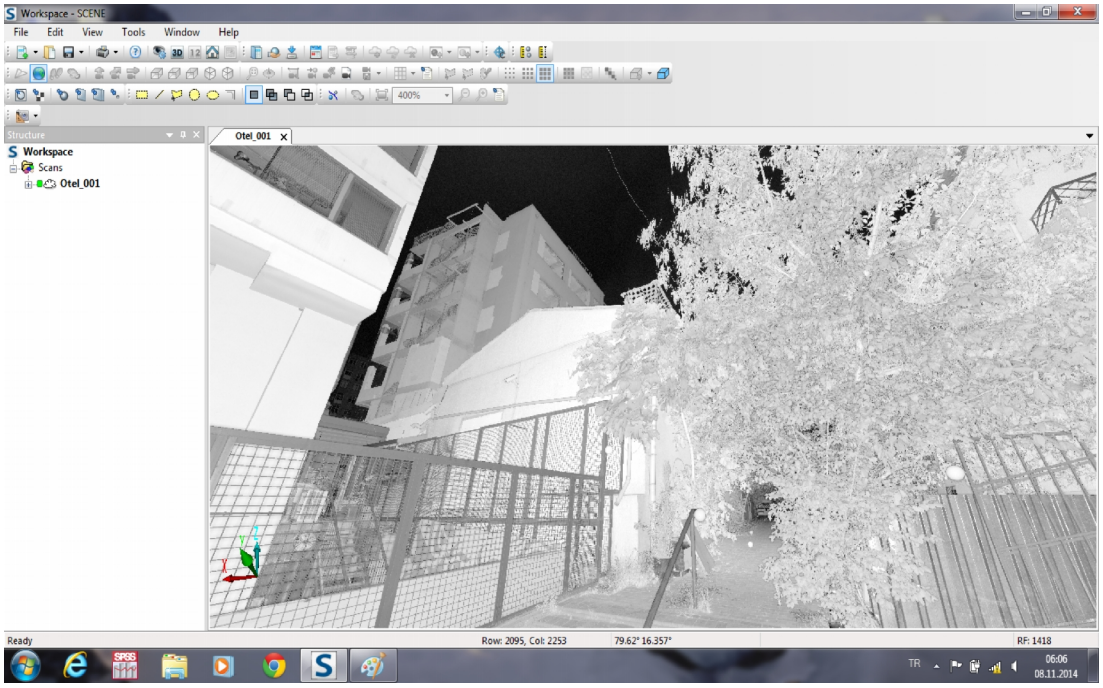


Fig. 2.4. Quick view of the scan building.

Since this is the starting point of the whole scanning, the FARO scanner can authomatically give a 001 scan name to this position. As explained in the

methodology section of this thesis, control points can either be a white ball or number written on an A4 / A3 paper. In this view you can notice control points been place in different positions. The FARO scanner whilst scanning, rotates at 360^0 horizontally and 320^0 vertically at every scanning point.

At the same position, Fig. 2.5. shows the planar view ;

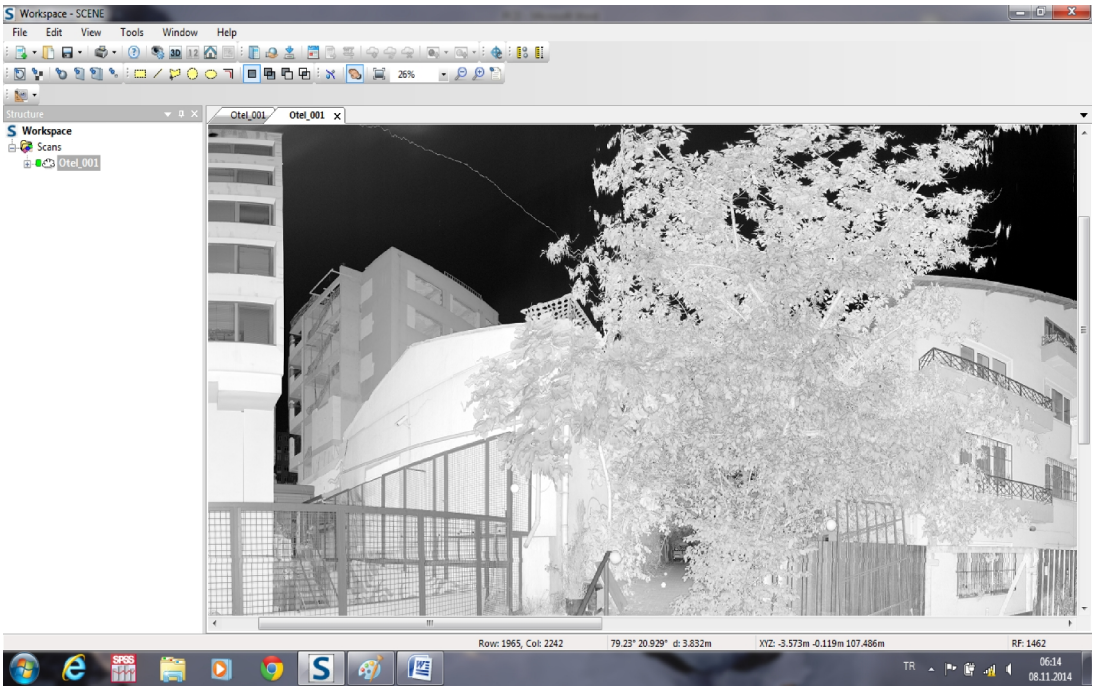


Fig. 2.5. Planar view of the building.

The planar view is actually use to detetermine a single scan. The laser scanner in general is "Inquisitive" , that is, it has the ability to scan any object(s) it comes in contacts with whilst in operation. This is one of the disadvantage of a laser scanner. For such reason it leads to the formation of millions of points since every object mean points. It has the capability to scan not less than fourty - thousands (40,000) points per second. In Geomatism, we see every point as significant. Whenever data exceeds ten-thousands (10,000), they become more significant.

Fig. 2.6. shows the 3D view of the building.

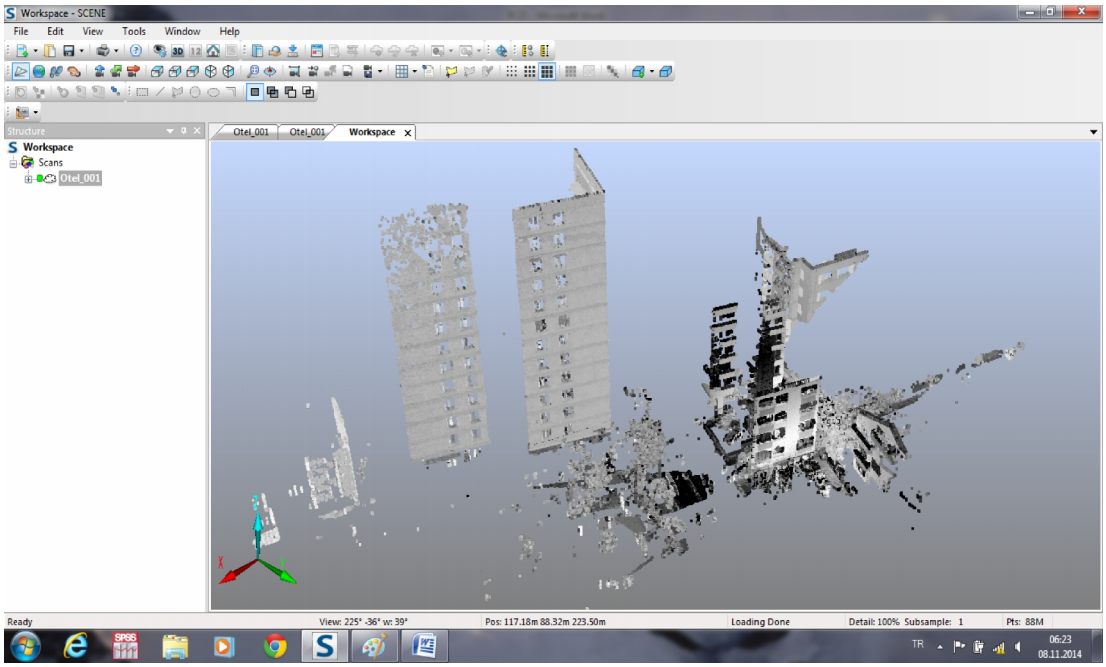


Fig. 2.6. 3D view of the building.

The 3D viewer is almost similar to reality. After proper analysis has been done on buildings, bridges, roads, dams and many more using the 3D viewer, we can easily be in a position to draw our inferences of wheather been deformed or not. To be precise, this is one of our main motive of scanning in Geomatism and also our objective in this thesis. This scanning is sometimes a repeated processes with the aim of arriving at a better conclusion.

Position 018 shows Quick view, planar view and 3D view of the upper part of the implemented building . You can see the different positions of the control points. Fig. 2.7.

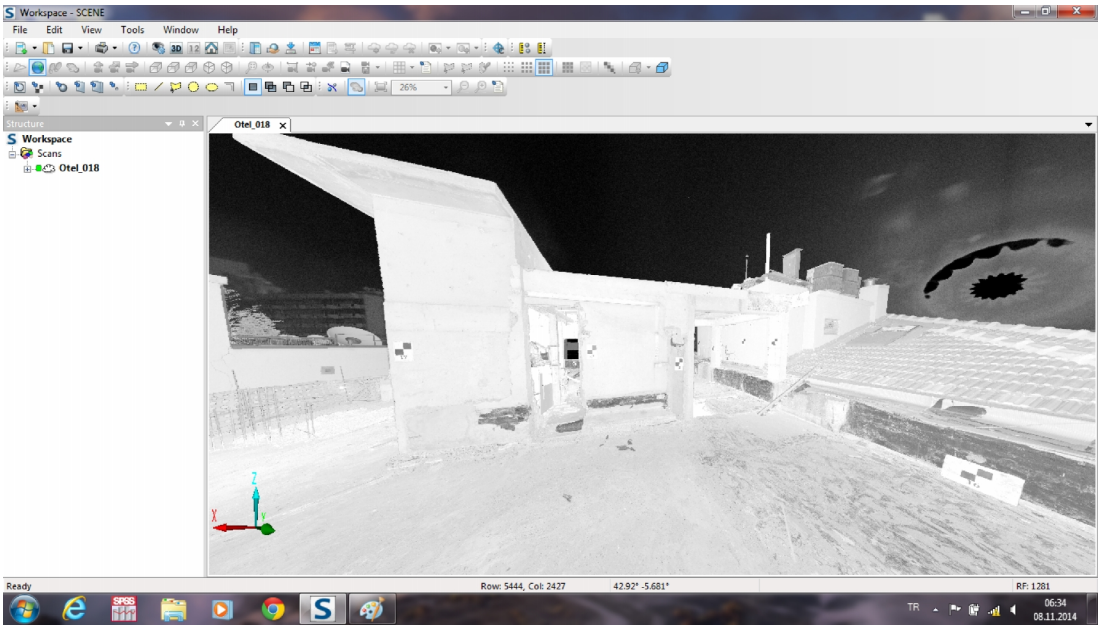


Fig. 2.7. Quick view of the upper part of implemented building.

Fig. 2.8;

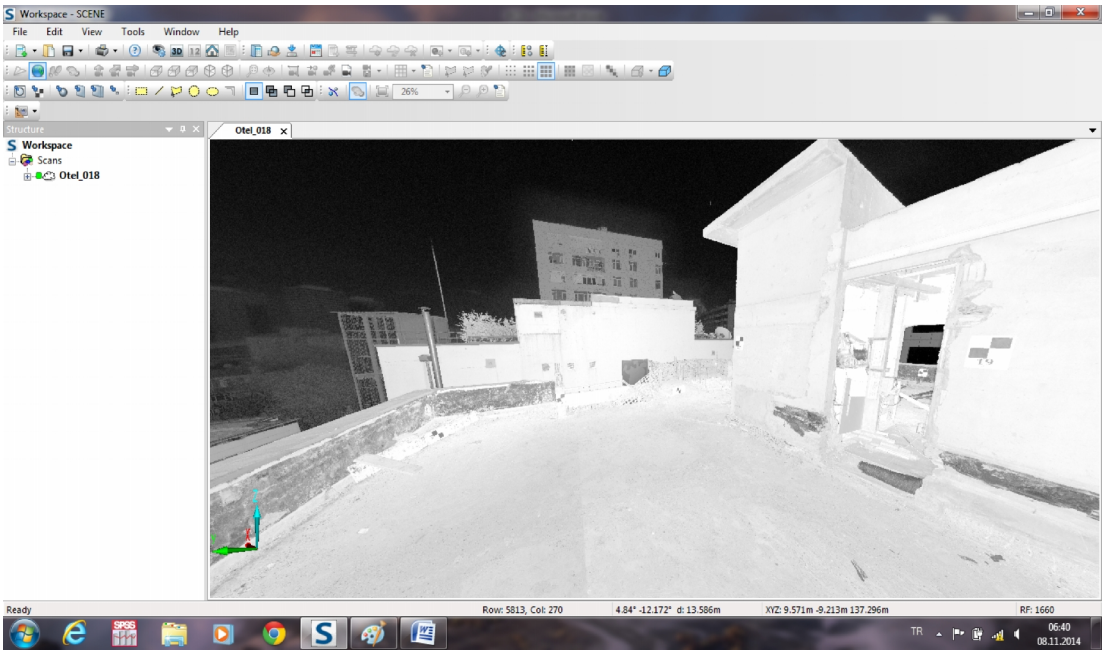


Fig. 2.8. Quick view of the upper part of implemented building.

Fig. 2.9;

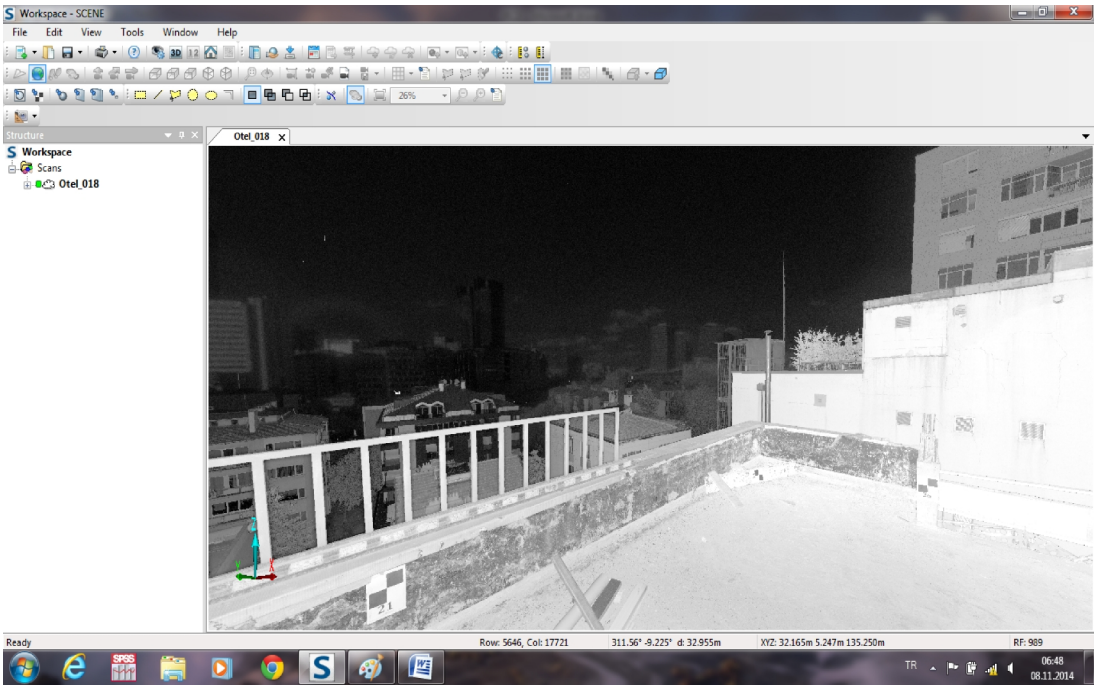


Fig. 2.9. Quick view of the upper part of implemented building.

Fig. 2.10;

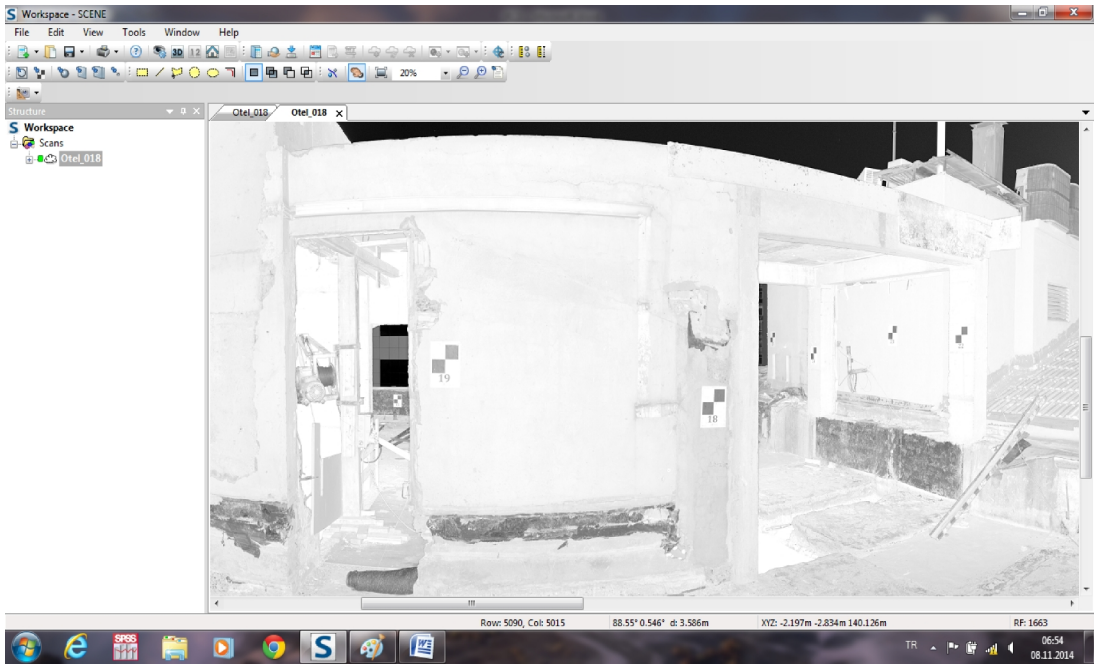


Fig. 2.10. Planar view of the upper part of implemented building.

Fig. 2.11;



Fig. 2.11. 3D view of the upper part of implemented building.

Fig. 2.12;

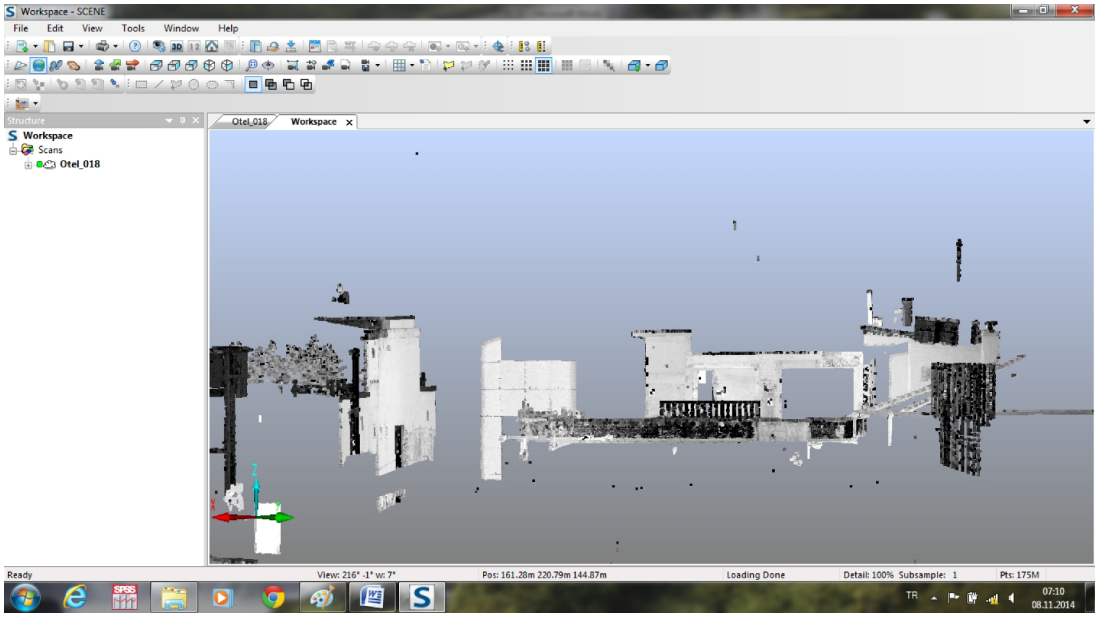


Fig. 2.12. 3D view of the upper part of implemented building.

Fig. 2.13;

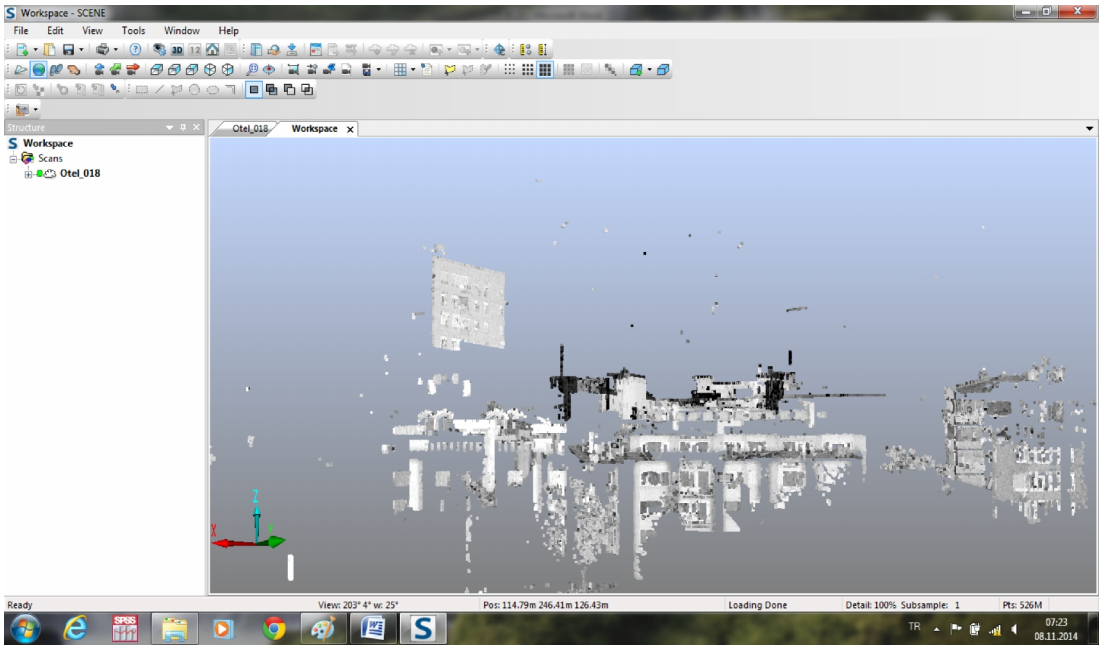


Fig. 2.13. 3D view of the upper part of implemented building.

Position 029 shows Quick view, planar view and 3D view of front view of implemented building . Fig. 2.14.

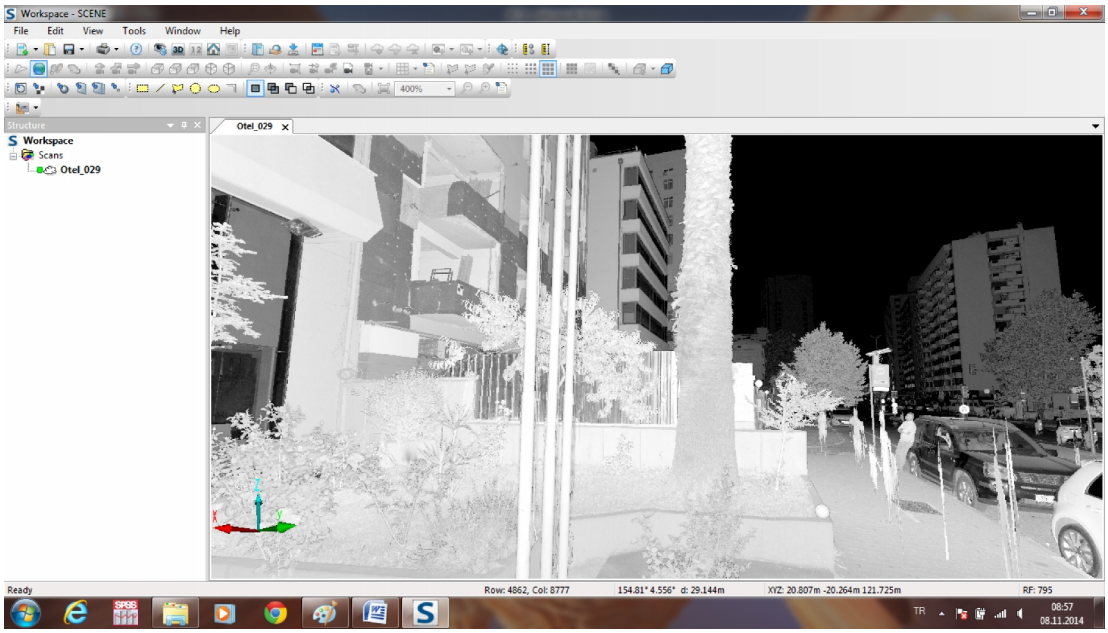


Fig. 2.14. Quick view of the front view of implemented building.

As you can see in the scan, there are a lots of polutions of human images which makes the scans noisy. If this unwanted points of images are not trace and remove (filter) from this scan can leads to larger amounts of errors. We generally prefered a scan to be done in conducive environment (e.g. night). Fig. 2.15. shows a planar view of the implemented building.

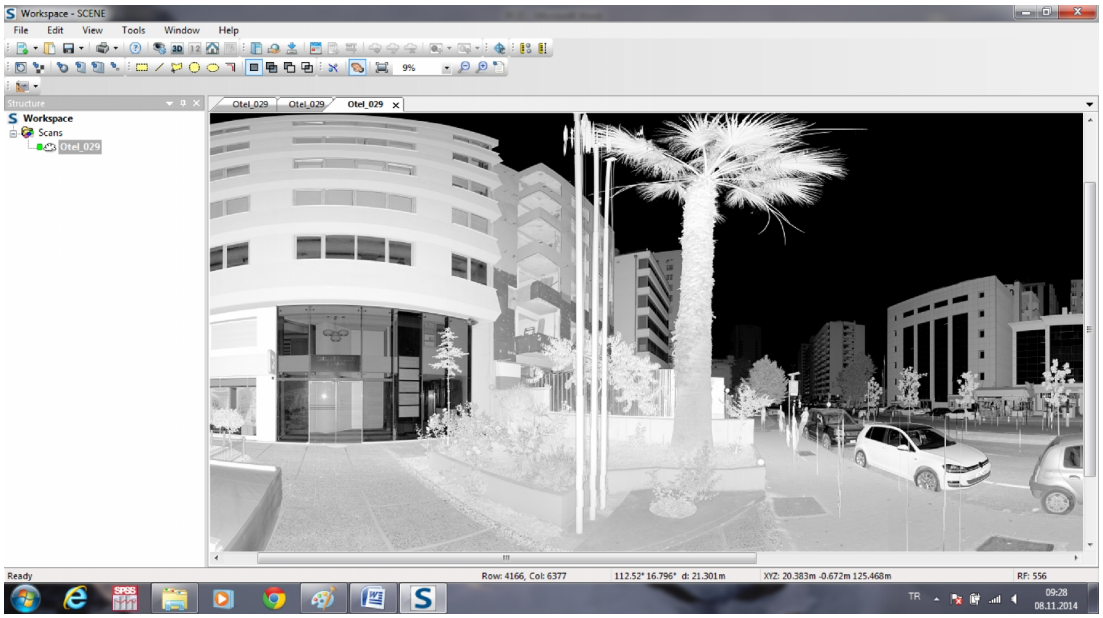


Fig. 2.15. Planar view of the front part of implementated building.

Fig. 2.16;

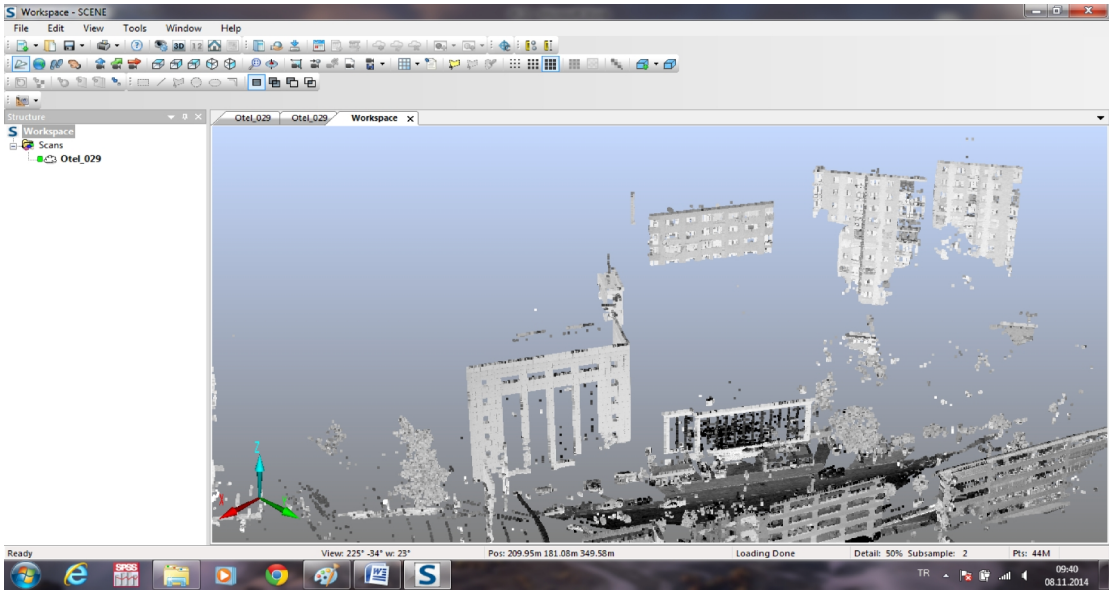


Fig. 2.16. 3D view of the front part of implementated building.

3. SURFACE MATCHING

As said earlier on, combining the advantages of LIDAR and stereo photogrammetry is an interesting fusion problem. In matching surfaces, we take into consideration the following; Encode distinctive local structure at a collection of image points for matching between images, despite modest changes in viewing conditions (changes in scale, orientation, contrast, etc.).

Key Issues:

- Feature point detection
- Feature descriptors
- Potential applications
    - Image panoramas (image matching and registration)
    - Long range motion (tracking by detection)
    - Stereoscopic vision / 3D reconstruction
    - Object recognition

Figure 3.1, 3.2, and 3.3, shows surface matching which leads to 3D reconstruction.



Fig. 3.1. 3D model from the left side



Fig. 3.2. 3D model from the right side



Fig. 3.3. Reconstructed 3D model

Feldmar and Ayache (1994a and 1994b) do not attempt strictly to find closest points, but to find closest feature vectors. See figure 3.4.



Fig. 3.4. With changes in scale, position, 3D viewpoint, and brightness

Multiple surface matching;

When more than two surfaces with multiple overlaps exist, the procedure is split into two steps: sequential pairwise registrations and a final global registration. The pairwise registrations establish the correspondences between the overlapping pairs of surfaces. The global registration distributes the residual errors evenly among all of the surfaces, and also considers the multiple overlap conditions and the closure condition, i.e. matching of the last surface to the first one. See figure 3.5



Fig 3.5. With changes in scale and position

One of the surfaces is selected as the reference,which defines the datum of the common coordinate system. The pairwise LS3D matching processes are run on every possible overlapping surface pairs, starting from the datum one. Each matched surface is incrementally added to the union of the previously registered surfaces. If the search surface is already in the union, i.e. surface has multiple overlaps, the transformation is not applied. Shown in the above figure 3.5.

Each pairwise registration gives the 3D transformation parameters of the search surface and additionally the correspondences between the template and the search surfaces. These final correspondences are saved to separate files. Every individual correspondence gives a (fictitious) tie point. The numbers of tie points are thinned out by selecting of every n-th correspondence.

Then, all these files are given as input to the block adjustment by independent models software BAM7, which is an in-house software based on a 7-parameter 3D similarity transformation. The block adjustment by independent models, which is a well-known orientation procedure in photogrammetry (Ackermann et al., 1973), was formerly proposed for the global registration of laser scanner pointclouds, but for the case of retro-reflective targets as tie points (Scaioni and Forlani, 2003).

In the BAM7 software, (fictitious) points of the datum surface are treated as the control points. This leads the transformation parameters of the datum surfaces fixed

in the procedure. The transformation parameters of all the other surfaces will be optimized regarding the global agreement of the whole data.

3.1 Transformation Selection

In linear regression, transformations of the predictor variables can often lead to more accurate predictions and a model that better fits the data. Many different transformation families have been suggested in the literature, along with a few methods for selecting a specific member of such a family. A non-Bayesian method was proposed in Box and Tidwell (1962), while Box and Cox (1964) discuss transformations with an emphasis on transforming the response variable. They also mention briefly a possible Bayesian approach. It appears, however, that the literature on Bayesian transformation methods is sparse at best. For a general treatment of transformations in regression, see Cook and Weisberg (1982), Carroll and Ruppert (1988), and the many references therein.

Laud and Ibrahim (1995) use a predictive criterion for selecting a specific member of a suitably chosen parametric transformation family. For this problem, a model $m \in \mu$ consists of a specific member of a given transformation family and is indexed by a vector of parameters $\boldsymbol{\alpha} = (\alpha_1, \ldots, \alpha_p)^T$. Thus;

$$\boldsymbol{Y} = \boldsymbol{X}_m \boldsymbol{\beta}^{(m)} + \boldsymbol{\epsilon}, \tag{3.1}$$

denotes a matrix of transformed predictors, and $\boldsymbol{\beta}^{(m)}$ is the vector of regression coefficients corresponding to $\boldsymbol{X}_m$.

A useful example of a family of transformations on a predictor **x** is the Box-Cox power family of transformations given by

$$g(\chi,\alpha) = \begin{cases} \dfrac{\chi^{\alpha}-1}{\alpha} & \alpha \neq 0 \\ \log(\chi) & \alpha = 0 \end{cases} \tag{3.2}$$

If one were to choose this family for each of the predictors, then for a given α, the ith row of $\boldsymbol{X}_m$ would be $\left(g(x_{i1};\, \alpha,), \ldots, g\left(x_{ip};\, \alpha_p\right)\right)$. One can also choose different families for different predictors, leading to $\boldsymbol{X}_m$ having ith row of the form $\left(g_1(x_{i1};\, \alpha,), \ldots, g_p\left(x_{ip};\, \alpha_p\right)\right)$.

Yet another possibility is to transform two predictors with a common parameter value from the same or different families. For instance, one may consider

two transformations, $\cos(\alpha t)$ $\sin(\alpha t)$, of the same variable t with a common parameter α, leading to $\boldsymbol{X}_n$ having ith row $(\cos(\alpha t_i), \sin(\alpha t_i))$. The predictive methods discussed here allow a great deal of exibility in principle. Further possibilities and more examples including variance stabilization are given in Laud and Ibrahim (1995).

In our case of transformation selection, we are interested in integrating 3D reconstruction of point clouds and solid models from LİDAR and digital stereo images. The space of comparison was based on the minimum processing of the data sets. Traditionally, comparison of digital surface models (DSM) data is based on establishing the point correspondence by establishing a common XY grid and derived the Z values of each DSM by interpolation. This will easily allows for the estimation of transformation selection between surfaces.

Another approach used for deriving the alignment between two point clouds is the Iterative Closest Point (ICP) method (Besl and McKay, 1992). It is an iterative procedure requiring good initial transformation values and it is based on the minimization of the distance between a point belonging to one data set and its closest points in the second data set.

3.1.1 Elaboration of Surface Representation And Similarity Criterion

Determines what type of information we extract from the 3D surfaces, which typically characterizes their local or global shape, and how we organize this information into a representation of the surface which will lead to improved efficiency and robustness in the last stage. In this thesis, surface representation and similarity criterion was mainly done by considering the following two criterion;

3D acquisition:

In order to analyze the surface of a real-world object in 3-dimensions, it must be scanned and converted into digital 3-dimensional data. Laser scanners are very common and highly accurate 3D acquisition tools (Parthasarathy et al. 1982; Sequeira et al. 1995; Marszalec & Myllyla 1997; Gokturk et al. 2004; Blais et al. 2007). The latter are able to produce high resolution, high accuracy scans. However they are usually expensive systems that take a long time to complete a full scan, and often require some mechanical system to move the laser and acquired readings before accumulation into a point cloud. For lower cost, lower scan times, and minimal mechanical complexity, stereoscopic vision systems are a very popular way

of digitizing a 3-dimensional scene (Murray & Jennings 1997; Murray & Little 2000; Se et al. 2001). If prominent features are lacking in a scene, such as on the surface of a smooth automotive body part, these construction techniques may fail due to a lack of usable points. One popular technique to overcome the limitations of using traditional stereoscopic imaging is to acquire 3-dimensional models using structured light scanners. This type of sensor projects a set of artificial features onto a model or scene that is being scanned, and then uses a vision system to acquire the model in 3D. Most structured lighting systems use a single camera along with a projector to acquire the 3D points (Rocchini et al. 2001; Zhang et al. 2002), or combine a pattern projector with a standard stereo pair of cameras to avoid calibration with the projector (Payeur & Desjardins 2009).

A recent trend in 3D sensing is the use of Microsoft's Kinect, which is a low-cost portable sensor that provides 3D visualization of a scene. Using structured light principles, an infrared laser projector generates artificial features onto a scene (which are invisible to the human eye), and a CMOS sensor reconstructs a scene through vision techniques. High quality scene reconstruction using the Kinect sensor has been studied (Shahram et al. 2011; Yan & Didier 2011). This analysis was done by instituting control points on various parts of the implemented building surface as a suitable means of 3D acquisition, the laser scanner (FARO laser scanner) remains to be the most accurate way to scan 3D models.

Deleting Unwanted Points (filtering):

Removing unwanted points is a central and an unavoidable process in preparing point cloud data for building model reconstruction, be it automatic or manual. This owes to the fact that, laser scanners lack the ability to selectively scan only the objects of interest. The resulting point cloud obtained from a laser scanner is thus a composition of points from objects within its field of view and focal range. While literature is lacking in methods for segregating off-terrain points into relevant and non-relevant points for a specified reconstruction work, numerous filtering algorithms that are devoted to automatic classification of point cloud into terrain and off-terrain points have been documented.

One group of these filters uses a mathematical morphology to filter out off-terrain points. A height difference is considered at each individual point and off-terrain points are identified as those with height differences above a certain predefined tolerance (Arefi & Hahn, 2005; Chen et al., 2007; Zhu et al.,

2011). Another group of filters is based on surface models. Ground points are filtered out by fitting a surface model through the entire point set that iteratively approaches the ground surface (Pfeifer et al., 1998). An in-depth review of these filters can be found in Meng et al. (2010).

Unfortunately, all these filters assume a particular structure of bare earth points in the surroundings of other object points. Morphological filters, for example is based on the basic assumption that buildings are higher than the neighboring topographic surface and that, there are no abrupt ground surface elevation changes in the buildings' neighborhood. Similarly, surface-model based algorithms assume that ground surfaces are usually smooth, without sharp corners on bare terrain surface features. Rarely are these assumptions about the terrain surfaces true. Ground surfaces are generally undulated. Even whereas they are paved, they can hardly be perfectly smooth and levelled. Moreover, a building may be constructed on a sloppy terrain. Because of these limitations, applying these filters to remove ground points may cause significant loss of relevant points which can hardly be recovered. In addition, due to the general irregular nature of the ground surfaces and the underlying assumptions of the automatic filtering algorithms, there is yet no filter that can remove all terrain points. Such leftover points have to be further cleansed manually.

Therefore, if accuracy is not to be compromised for automation, removal of irrelevant points is better done manually. Manual removal of irrelevant points, as done in this research, basically entails visually identifying such points, manually selecting and deleting them. Because a terrestrial scanner is usually stationed at different locations in order to obtain a complete scan of a building, this process is done on every individual scan to obtain roughly cleanse data before registration.

3D acquisition and Deleting Unwanted Points (filtering), was used in this thesis to elaborated that surface can only match when they are similar, this can be shown in surface representation of fig. 3.4 and 3.5 of this thesis.

3.1.2 Matching Establishment

A confusion matrix can be formed by computing the distance between each model Local shape descriptor (LSD) with each image LSD. Rows and columns of this matrix correspond with model and image LSDs respectively. There are various

ways for selecting candidate point matches from a confusion matrix (equations; 2.3 and 2.4). One way is to select the top model descriptor for each image descriptor by finding the maximum value of each column. Another is to select point correspondences that result from unambiguous LSD matches. The latter method is often superior as it could account for the fact that some image LSDs do not correspond to any model LSDs, e.g. those that correspond to scene clutter. This can be seen in fig. 3.4 and 3.5. of this thesis wherein you can see clutter of point clouds of building.

The rigorous method for selecting such unambiguous matches is to search for columns that have a maximum that is sufficiently larger than the rest of the values in the column, such that it stands out in a statistically meaningful sense (2.4). Since this is computationally costly, a simple approximation could be used that only requires comparing the maximum value (I_1) with the second largest value (I_2) (Fig. 2.1). A match is then established between model and image LSDs only if I_1 is sufficiently larger than I_2, that is, $s = (I_1 - I_2)I_1$ is greater than a predetermined threshold value s_t. For computational efficiency, it is not necessary to compute the confusion matrix in its entirety and at most finding the two nearest neighbours of each LSD is sufficient.

4. SURFACE RECONSTRUCTION

With surface reconstruction we refer to the process of deriving features in the 3D object space. The traditional method of reconstructing surfaces is by photogrammetry. Here, a feature on the ground, say a point or a linear feature, is reconstructed from two overlapping aerial images—a process known as stereopsis. This requires the identification of the ground feature in both images as well as the exterior orientation of the images. The crucial step in stereopsis is the identification of the same ground feature, also referred to as correspondence problem or image matching. Human operators are remarkably adept in finding conjugate (identical) features. DEMs generated by operators on analytical plotters or on softcopy workstations are of high quality but the process is time and cost intensive. Thus, major research efforts have been devoted to make stereopsis an automatic process.

Despite considerable research efforts there is no established and widely accepted method that would generate surfaces in more complex settings, say large-scale urban scenes, completely, accurately, and robustly. A human operator needs to be involved, at least on the level of quality control and editing.

On the other hand, LIDAR has been touted as a promising method to capture digital elevation data effectively and accurately. LIDAR can be viewed as a system that samples points of the reflective surface of the earth. The samples are irregularly spaced. You can see the original surface measurements point cloud or mass points in fig. 3.4 and Fig. 3.5 of this thesis . Laser points are computed from navigation data (GPS/INS) and range measurements. It is important to realize that there is no inherent redundancy in the computation of a laser point. In general, laser points do not carry semantic information about the scene.

4.1 Implicit vs Explicit Surface Description

Common to the techniques of acquiring digital elevation data is a cloud of 3D points on the visible surface. Except for measuring DEMs on analytical plotters, the mass points are irregularly distributed. Consequently, the next step is to interpolate

the raw points into a regular grid. Digital Elevation Models (DEM) are immensely popular in many engineering applications. With DEM we refer to a surface representation with bare-earth z- values at regularly spaced intervals in x- and y-direction. A bare-earth DEM is void of vegetation and man-made features—in contrast to a Digital Surface Model (DSM) that depicts elevations of the top surfaces of features elevated above the bare earth. Examples include buildings, vegetation canopies, power lines, and towers. Finally, the term Digital Terrain Model (DTM) is used as a DEM, augmented with significant topographic features, such as breaklines and characteristic points. A breakline is a linear feature that describes a discontinuity in the surface. Such discontinuities may signal abrupt changes in elevations across the breakline, or may refer to abrupt changes of the surface normal.

Although very useful, it is important to realize that a DEM or DSM does not make surface properties explicit. An explicit description of surface characteristics, such as planar or higher-order surface patches, surface discontinuities and surface roughness, is important for most subsequent tasks. Object recognition and image understanding rely on the knowledge of explicit surface properties and even the generation of orthophotos would greatly benefit from an explicit description of the surface. In this line of thinking we consider DEMs and DSMs as entirely implicit surface descriptions and DTMs as partially explicit (if breaklines and distinct elevation points are present). The challenge of describing the surface explicitly can be met easier if aerial imagery and LIDAR point clouds are fused. As described in Lee (2002), the generation of explicit surface descriptions from irregularly distributed mass points is accomplished by way of segmentation and grouping processes, embedded in the theoretical framework of perceptual organization.

4.1.1 Orientation Based on 2D Image Edges and 3D LİDAR Edges

Several researchers in photogrammetry and computer vision have proposed the use of linear features in form of straight lines for pose estimation. Most solutions are based on the coplanarity model. Here, every point measured on a straight line in image space gives rise to a condition equation in that the point is forced to lie on the plane defined by the perspective center and the control line in object space, see, e.g.Habib et al.(2000). The solutions mainly differ in how 3D straight lines are represented.

Although straight lines are likely to be the dominant linear features in this fusion problem, it is desirable to generalize the approach and include free-form curves. Zalmanson (2000) presents a solution to this problem for frame cameras. In contrast to the coplanarity model, the author employs a modified collinearity model that is based on a parametric representation of analytical curves. Thus, straight lines and higher-order curves are treated within the same representational framework.

With the recent emergence of digital line cameras it is necessary to solve the pose estimation problem for dynamic sensors. The traditional approach is a combination of direct orientation and interpolation of orientation parameters for every line. This does not solve our fusion problem because no correspondence between extracted features from LIDAR and imagery is used—hence no explicit quality control of the sensor alignment is possible. In Lee, Y. (2002) the author presents a solution of estimating the pose for line cameras by using linear features. In this unique approach every sensor line is oriented individually, without the need for navigation data (GPS/INS).

4.1.2 Orientation Based on 3D Model Edges and 3D LIDAR Edges

The addition of fusion with 3D model edges are more for the purpose of completeness than practical significance. In contrast to the previous method, edges must be matched between images to obtain 3D model edges. In general, image matching, especially in urban (İstanbul) areas, is considered difficult. We should bear in mind, however, that in our fusion problem, the surface can be considered to be known (Fig. 3.4 and Fig. 3.5). Hence, the problem of geometric distortions of features can be well controlled and matching becomes feasible, assuming that reasonable approximations of the exterior orientation parameters are available. In fact, matching in object space, using iteratively warped images, becomes the method of choice. This matching procedure also offers the opportunity to match multiple images. Now we have the chance for a detailed reconstruction of complex surfaces from multiple images. Using the implementation building and analysis of Fig. 3.4 and Fig. 3.5. of this thesis you can attest to the fact that several surfaces were scanned inorder to make a fusion.

4.1.3 Orientation With Surface Patches

Originally, the idea of using surfaces in the form of DEMs for orienting models was suggested by Ebner and Strunz (1988). The approach is based on minimizing the z−differences between the model points and points in object space found by interpolating the DEM. The differences are minimized by determining the absolute orientation parameters of the model. Schenk(1999a) modified the approach by minimizing the distances between corresponding surface elements.

The advantage of using patches as sensor invariant features is the relatively simple process to extract them from laser points. The fitting error of the laser points to a mathematical surface serves as quality control measure. In contrast to the previous methods, no planimetric features need to be extracted. Patches are more robust than features derived from them, for example 3D edges.

Unfortunately, the situation is quite different for determining surface patches in aerial images. Although theoretically possible by texture segmentation and gradiant analysis, it is very unlikely that surface information can be extracted from single images. Hence, image matching (fusion) is required. Quite often, surface patches have uniform reflectance properties. Thus, the grey level distribution of conjugate image patches is likely to be uniform too, precluding both, area - based and feature-based matching methods, respectively. The most promising approach is to infer surface patches from surface boundaries (matched edges).

As shown by Jaw (1999), the concept of using control surfaces for orienting stereo models can be extended to block adjustment. In analogy to tie points, the author introduces tie surfaces. To connect adjacent models, the only condition is to measure points on the same surface. However, the points do not need to be identical—clearly, a major advantage for automatic aerial triangulation.

4.1.4 Alternative Solution With Range Images

A popular way to deal with laser points is to convert them to range images. This is not only advantageous for visualizing 3D laser point clouds but a plethora of image processing algorithms can operate on range images. For example, an edge operator will find edges in a range image, suggesting that the 3D edges used as sensor invariant features be determined from range images. At first sight, this is very

appealing since it appears much simpler than the method described in Section 1.1 Let us take a closer look before making a final judgment, however.

Generating range images entails the interpolation of the irregularly spaced laser points to a grid and the conversion of elevations to grey values. While the conversion is straightforward, the interpolation deserves closer attention. Our goal is to detect edges. Edges in range images correspond to rapid changes of elevations in the direction across the edge. This is precisely where we must expect large interpolation errors. It follows that the localization of edges in range images may not be accurate enough for precise fusion. Figure 3.4. and Fig. 3.5. of this thesis wherein you can see analysis and matching of surfaces.

4.2. Surface Patches

Are obtained by segmenting the laser point cloud. The segmentation process will leave gaps, that is, patches do not contiguously cover the visible surface. A variety of reasons contribute to this situation. For one, occlusions and low reflectance (e.g. water bodies) result in regions with weakly populated laser points. Moreover, certain surfaces, such as the top of canopies, or single trees and shrubs do not lend themselves to a simple analytical surface description. It is conceivable to augment the set of surface patches obtained from LIDAR data by surfaces obtained from aerial imagery. An interesting example is vertical walls, such as building facades. The number of laser points reflected from vertical surfaces is usually below the threshold criterion for segmentation. It is therefore very unlikely that vertical surface patches are extracted. During the analysis of spatial relationships among patches it is possible to deduce the existence of vertical patches. These hypotheses can then be confirmed or rejected by evidence gained from aerial images.

4.2.1 Normal and Curvature Estimation

Reliable estimation of geometric properties such as normal vectors and curvatures of discrete data point is a fundamental task in many applications and across many walks of life; because they serve various purposes. Typical applications that use these geometric properties include point cloud segmentation (Rabbani et al., 2006), surface reconstruction (Amenta & Bern, 1999; Kazhdan et al., 2006), point cloud registration (Gressin et al., 2013). Many other example applications

across multiple disciplines can be found in Page et al. (2002). As a result, this topic is well researched and documented in literature.

There are basically two different approaches for estimating normals and curvatures of discrete data points sampled from a real world object.

- Reconstruct / triangulate the points to identify the neighboring points that characterize the local geometries of the surfaces the points represent, and then estimate the parameters therefrom.
- Estimate the parameters directly from the point cloud by fitting directional tangent vectors to the data points; i.e., fitting a tangent plane or a quadric surface to each point and its local neighbors.

Comparative reviews on these two approaches are given in Jin et al. (2005) and Meek and Walton (2000). Here, the triangulation-based approach is utilized for the reason that, building edge and boundary points can be identified and extracted during this process. Extraction of edge points is essential to the proposed hole-feeling strategy.

To estimate the normal vector and curvature of a point from triangulation, supposed that the point whose normal is to be determined is v, and a local mesh / triangulation composing of v is available, we collect triangular faces that constitute 1-ring neighborhood of v as shown in the figure 4.1. Note that, to follow the normal convention, throughout this section, v (vertex) will be used to refer to a point in a triangulation, and p, to a point in the point cloud.

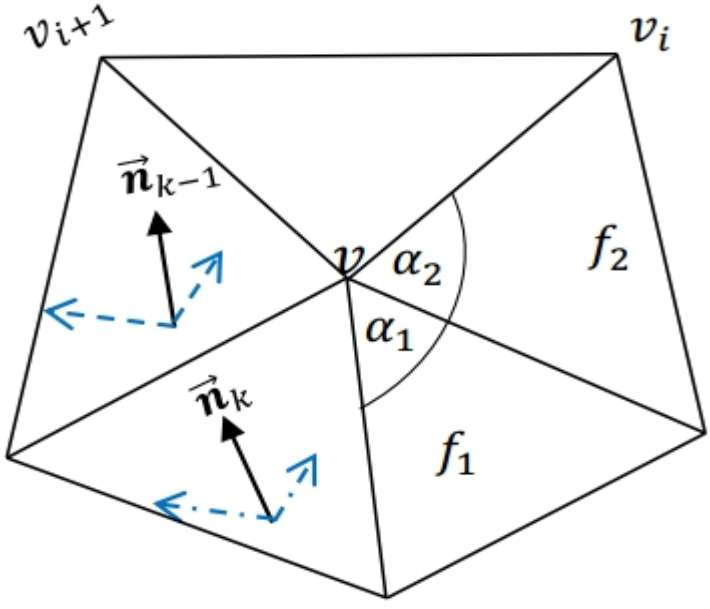


Fig. 4.1. Estimating normal vector and curvature of vertex v

The normal vector $\boldsymbol{n}$ of **v** is computed using angle-weighted average method (Thürrner & Wüthrich, 1998) as follows:

$$n = \frac{\sum_{i=1}^{k} W_i n_i}{\sum_{i=1}^{k} W_i} \tag{4.1}$$

where,

$\boldsymbol{n}$ is the normalized normal vector of the individual incident triangular faces f_i,

$\mathbf{W_i} = < v_i v v_{i+1} = \alpha_i$ is the weight of f_i, and

K = number of triangular faces incident on **v**

The curvatures are estimated as follows (Meyer et al., 2003):

$$K_{G_i} = \frac{2\pi - \sum_{i=1}^{k} \alpha_i}{A_{mixed}} \tag{4.2}$$

where,

α_i and **K** are defined as above and

A_{mixed} is the area of 1-ring neighborhood of **v**, over which the curvature is estimated.

The definition of A_{mixed}, and how it is computed are discussed in detail in Meyer et al. (2003). It is sufficient to state here that it is a weighting factor.

This algorithm for computing a normal vector and a curvature of a given vertex from a discrete triangulation, using equations (4.1) and (4.2) are discussed in detail in Meyer et al. (2003). From Figure 4.1, it will be noticed that, using these equations requires a 1-ring neighborhood of a vertex v, from an existing triangulation. However, up this stage of our data processing, the input data is still in a point cloud domain. This means, in order for the discussed algorithms to be applied, an existing triangulation containing a vertex v must be made available, from which a 1-ring neighborhood of v can be identified. To accomplish this, a local Delaunay triangulation is built from neighboring points that most suitably described the underlying local surface around the point under consideration. Then the vertex v, corresponding to the point under consideration is located on the resulting triangulation. Once this vertex is found, its 1-ring neighborhood faces are identified as shown in the figure 4.1. From this 1-ring

neighborhood, a vertex normal and curvature are estimated using equation (4.1) and (4.2) as shown in appendix D of Lamin O. Ceesay Masters thesis 2014. To estimate the normal vectors and curvatures of all the points in the input point cloud data set, these steps are repeated for each point as shown in appendix C of Lamin O. Ceesay Masters thesis 2014.

It is worth noting that, the selection of the nearest neighbors needs a careful consideration. Reliable estimation of normal vector and curvature of a point within a point cloud is much dependent on the points that participated in the estimation. With a uniform point sampling density or an organized point cloud, one could simply choose a fixed number of points that are nearest to a point **P**, and be almost sure of having points distributed on all sides of **P**. But in most real cases, point clouds are of varying densities and unorganized. As a result, when a fixed value is used for neighborhood selection, **P** might be located on one side of the selected points. Using only points from one side of P may not give a good approximation of the local geometry of the surface around **P**. One fix to this is to use a value large enough. However, from computation efficiency point of view, this is not a good idea. Therefore, in order to be highly certain that P is almost always centered among the selected neighboring points (with the exception of the boundary points) and also to account for the surface roughness, a well strategized neighborhood selection is used. The local neighbors of a point are determined within a region bounded by two spheres of radius R_1 (outer sphere) and R_2 (inner sphere), both centered on P_i as shown below.

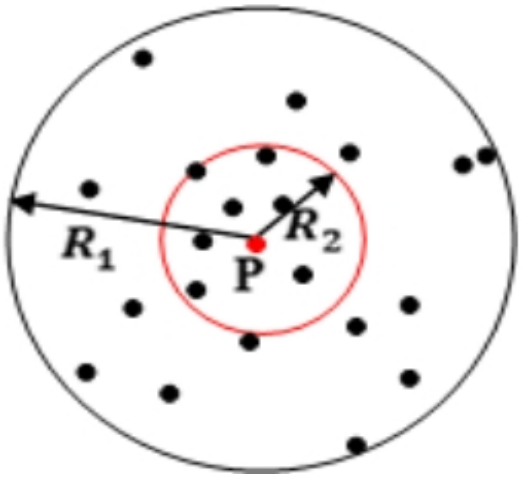


Fig. 4.2. Neighborhood selection for point P

R_1 controls the area of the region around **P**, over which normal and curvature are determined, and R_2 accounts for noise and roughness of the surface in the immediate surroundings of **P**. R_2 is not strictly needed if the scanned building surfaces are smooth and the data set is less noisy ; in which case, it can be set to zero. Ideally, R_1 should be sufficiently small that estimation is done as locally as possible, but large enough to allow points to be selected on all sides of **P**. On the other hand, R_2 should be large enough to filter out points that almost coincided with **P**, but sufficiently small to allow for detection of transitions from smooth surfaces to sharp edges.

The term Sharp edges can be considered as an abstraction in the context of real world buildings. Most building edges in the real world are chamfered. In other words, most building surfaces in the real world are connected by blended edges rather than completely sharp ones. In these cases, R_2 can also serve as a sharp feature sensitive metric which will lend its advantage to the proposed edge extraction method. Depending on the density of the point cloud, different values of R_1 and R_2 can be chosen. So, in order to be flexible, it is considered prudent to leave the selection of these values to the judgment of the user. They are therefore left as user inputs, so they can be adjusted and fine-tuned to the user's satisfaction.

4.2.2 Boundaries

It is assumed that surface patches correspond to physical surfaces in object space. As such, they are only relevant within their boundaries. Thus, the complete boundary description,B, is important. The simplest way to represent the boundary is by a closed sequence of 3D vectors. The convex hull of the laser points of a surface patch serves as a first crude estimation of the patches' boundary. It is refined during the perceptual organization of the surface. However, boundaries inferred from LIDAR data remain fuzzy because laser points carry no direct information about boundaries. A much improved boundary estimate can be expected from aerial imagery. Matching extracted edges in two or more overlapping images is greatly facilitated by the LIDAR surface and by the knowledge where boundaries are to be expected. Thus it stands to reason to replace the somewhat fuzzy boundaries obtained from LIDAR by 3D edges derived from aerial imagery.

4.2.3 Identifying Boundary and Edge Points

In past years, many efforts have been put into the line feature extraction from range data sampled from a surface. However, most of the past research efforts concentrated on the extraction from polygonal surface meshes such as, in Meyer and Marin (2004) and Galantucci and Percoco (2005). In building model reconstruction, these methods are only useful for high level or intermediate processes such as surface refinement or conversion from a lower to a high level representation. For the proposed reconstruction method, extraction methods that work directly on the point cloud are more attractive, as the results can be used to support the intended early processing step, i.e., point cloud segment decomposition.

Some building reconstruction works fit plans to the point cloud and intersect the adjacent planes. Building edges are identified as the lines defined by the intersections of the planes (Stamos & Allen, 2000), or the bounding box of the fitted planes (Zhu et al., 2011). Depending on the fitting accuracy of each plane, the line of intersection between two planes can severely deviate from the actual building edge, both in position and in orientation. Moreover, this approach will produce a lot of fictitious lines from the intersection of non-neighboring planes.

Some others have taken a different approach. They extracted edges and boundaries from the point cloud, by converting it into range images and applying some well-known image based edge extraction methods such as, Sobel operator, Canny edge detector, etc. (Ali et al., 2008; Becker & Haala, 2007). However, similar to the planar fitting methods, due to the lower resolutions of range images generated from point clouds, this approach may produce lots of spurious lines, and in some case, some important line features may not be extracted. Furthermore, this forward and backward conversion between 3D and 2D point representation can cause a significant information loss.

Apparently, it appears that none of these approaches suits our convenience. This is not only because of the quality of the outputs, but also, they will require an additional processing stage in the proposed reconstruction of 3D. Therefore, a different approach is taken in this research. The most important thing about the

proposed approach is that, it is effective and it does not need to be executed as a separate processing step. It is easily incorporable into the normal estimation process. The rest of this section describes the proposed extraction method.

The constellation of triangles used for normal estimation can be used to identify potential boundary and sharp feature points. The term sharp features will be used here to refer to building edges and corners. A point is identified as a boundary point, if at least, one of its incident triangular faces has an edge that it does not share with any other face in the initial triangulation of P and its neighbors. It should be pointed out that though, this is a well established concept. In fact, most of the specialized mesh based hole filling algorithms use this concept to identify holes on mesh base surfaces. The same concept is simply used here to identify points on the building boundaries; by applying it to the locally approximated surface at each data point. However, for identifying edge points, a totally different concept is used. As it will be discussed next, this is a very intuitive, a simple and yet, a very effective approach.

Given a point cloud $\mathbb{P}$, sampled from a building surface S, let S_i be a sub-surface on S approximated by the neighborhood of point P_i in $\mathbb{P}$ and let $\sum F_j$ be a discrete triangular representation of S_i in which each triangular face F_j is incident on P as shown in figure 4.2. The goal is to detect if $\sum F_i$ contains a sharp feature. In other words, to determine if P_i corresponds to a sharp feature point on S. One intuitive and quite straightforward approach to do this, is to consider the dihedral angles between the adjacent faces, i.e., the interior angles at the edges between adjacent faces as shown in figure 4.3.

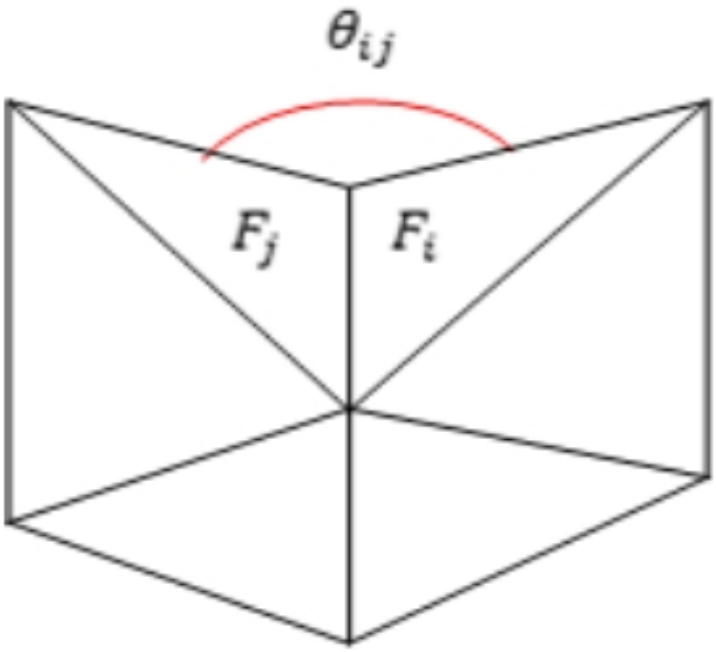


Fig. 4.3. Interior angle between adjacent faces of a triangular mesh

Since the measure of the dihedral angle between two intersecting planes (note that each non-degenerate triangle in space defines a plane) is a supplementary measure of the angle between their normal vectors, the problem is reduced to commutating the angles between the normal vectors of adjacent faces. Let $\boldsymbol{n}$ and $\boldsymbol{n}$ be the unit normal vectors to the planes of two adjacent faces F_i and F_j respectively and let θ_{ij} denotes the dihedral angle between them. For two adjacent faces that are on the same flat surface, we defined θ_{ij} as π. Based on this definition, the value of θ_{ij} will get smaller as the two adjacent faces deviate from a common plane. This is a valuable cue that is used to decide if a point is a sharp feature point or not. After determining the dihedral angle between each pair of adjacent faces, the smallest of these values is compared with a user specified threshold θ_{th}. That is:

$$\theta \coloneqq \min(\theta_{ij}) \tag{4.3}$$

If $\boldsymbol{\theta}$ is smaller than θ_{th}, then $\sum \boldsymbol{F_i}$ is considered to contain a sharp feature; or alternatively stated, $\boldsymbol{P_i}$ is categorized as a sharp feature point and is tagged as so. The threshold $\boldsymbol{\theta_{th}}$ accounts for the noise, and it also serves as a sensitivity measure that helps distinguish sharp feature points from those located on curved surfaces other than sharp features. This algorithm is simply incorporated into

normal estimation process as shown in appendix D and appendix C of Lamin O. Ceesay Masters thesis 2014.

4.2.4 Discontinuities

Are linear features in object space that signal either an abrupt change in the surface normal or an abrupt change in the elevation. Discontinuities constitute very valuable information, not only for automatic scene interpretation but also for mundane tasks such as the generation of orthophotos. Like boundaries, discontinuities are represented as 3D polylines. With a few exceptions, boundaries are, in fact, discontinuities. Whenever patches are adjacent their common boundary must be a discontinuity. Take a saddle roof, for example. If the adjacency of the two roof planes is confirmed then their common boundary (e.g. intersection of roof planes) is a discontinuity. Since discontinuities are richer in information than boundaries, it is desirable to replace boundaries whenever possible by discontinuities.

Discontinuities are derived from aerial images in the same fashion as boundaries. Moreover, some of them can be obtained from LIDAR by intersecting adjacent surface patches. As noted earlier, corresponding 3D edges from images and 3D edges from LIDAR are used for establishing a common reference frame between images and LIDAR.

4.3 Roughness

Is a surface patch attribute that may be useful in certain applications. It can be defined as the fitting error of the surface patch with respect to the laser points. The waveform analysis of returning laser pulses yield additional information about the roughness of the laser footprint and hence the surface patch.

5. CASE STUDY

In this thesis work, five of the scan surfaces were taken into consideratiıon. They are as follow;

Scan 001 in 3D view:

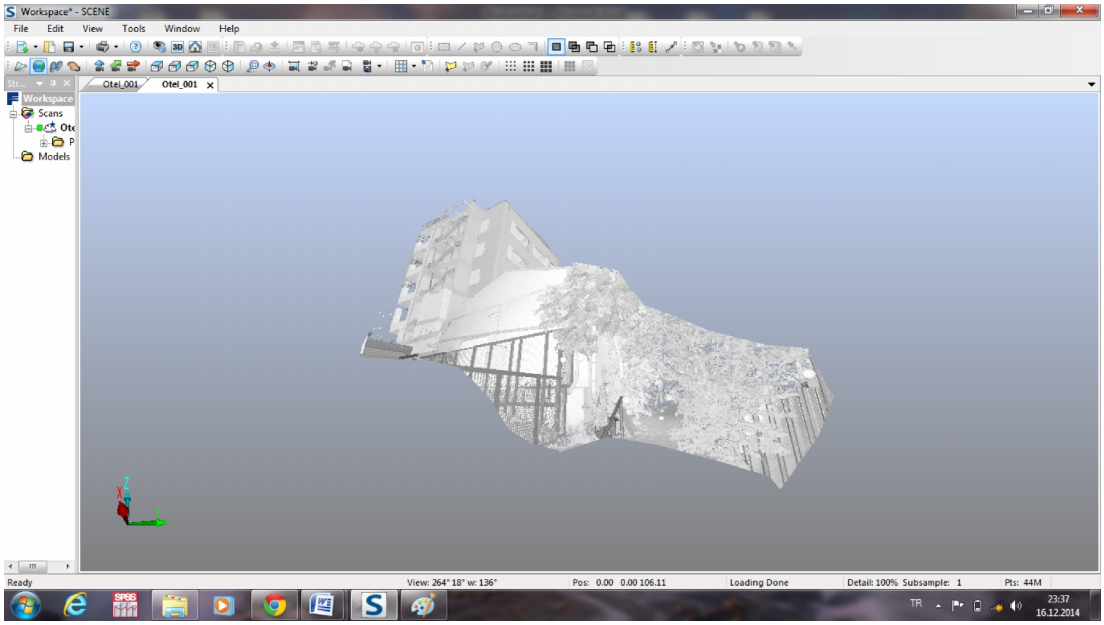
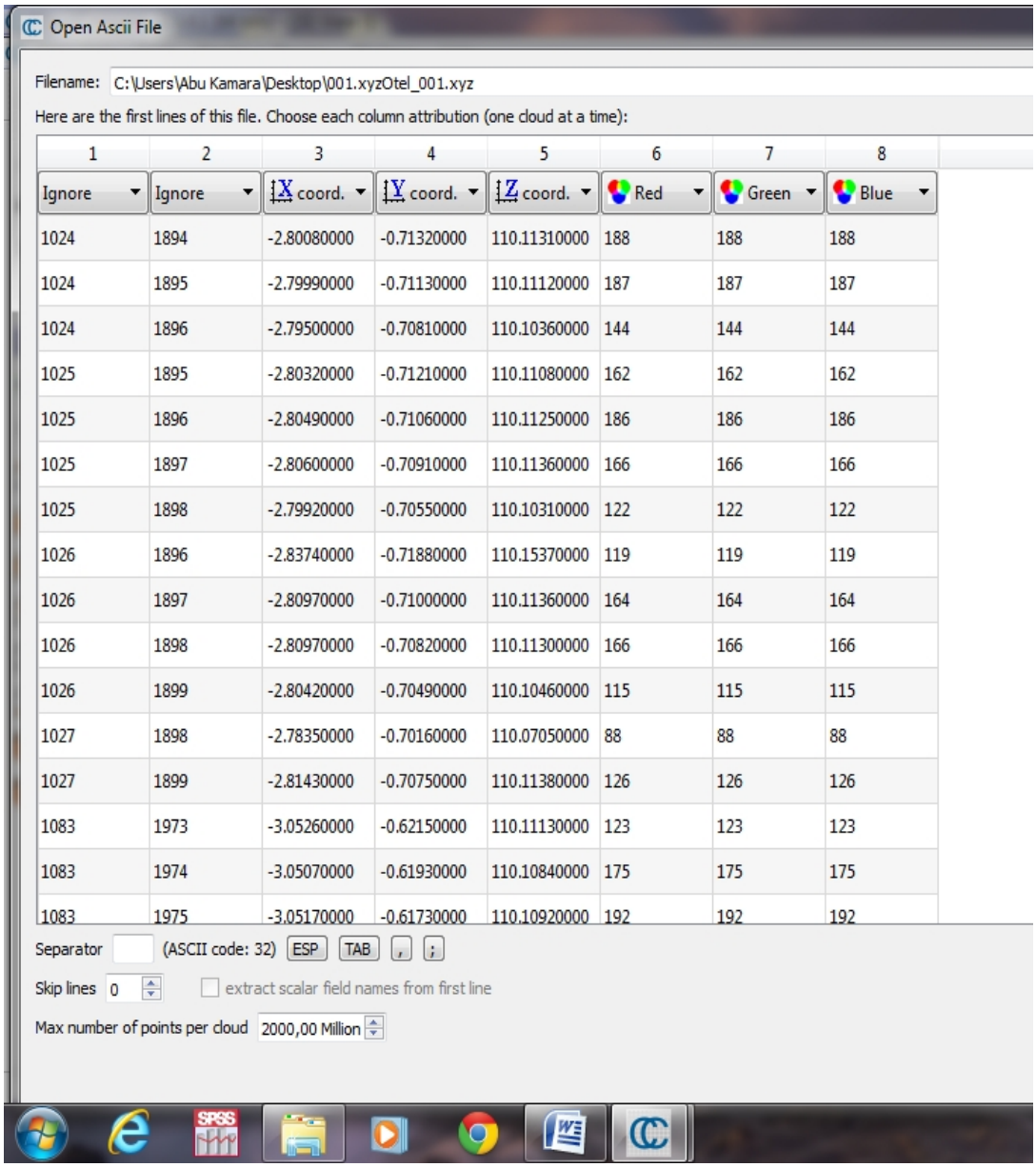


Fig. 5.1. 3D view of the implemented building.

3D view of the building with area of control points after filteration. The scan coordinates (points) of this surface is in Fig. 5.2. This points were collected from faro scan and saved into Ascii (x, y and z) file format, cloudcompare was used to open the data.



1	2	3	4	5	6	7	8
Ignore	Ignore	X coord.	Y coord.	Z coord.	Red	Green	Blue
1024	1894	-2.80080000	-0.71320000	110.11310000	188	188	188
1024	1895	-2.79990000	-0.71130000	110.11120000	187	187	187
1024	1896	-2.79500000	-0.70810000	110.10360000	144	144	144
1025	1895	-2.80320000	-0.71210000	110.11080000	162	162	162
1025	1896	-2.80490000	-0.71060000	110.11250000	186	186	186
1025	1897	-2.80600000	-0.70910000	110.11360000	166	166	166
1025	1898	-2.79920000	-0.70550000	110.10310000	122	122	122
1026	1896	-2.83740000	-0.71880000	110.15370000	119	119	119
1026	1897	-2.80970000	-0.71000000	110.11360000	164	164	164
1026	1898	-2.80970000	-0.70820000	110.11300000	166	166	166
1026	1899	-2.80420000	-0.70490000	110.10460000	115	115	115
1027	1898	-2.78350000	-0.70160000	110.07050000	88	88	88
1027	1899	-2.81430000	-0.70750000	110.11380000	126	126	126
1083	1973	-3.05260000	-0.62150000	110.11130000	123	123	123
1083	1974	-3.05070000	-0.61930000	110.10840000	175	175	175
1083	1975	-3.05170000	-0.61730000	110.10920000	192	192	192

Fig. 5.2. scan points of 001 surface

The first two coloumns represent position, followed by x, y, and z coordinates of the scan points. The last three digit represent the color red, green and blue (RGB).

Scan 006 in 3D view:

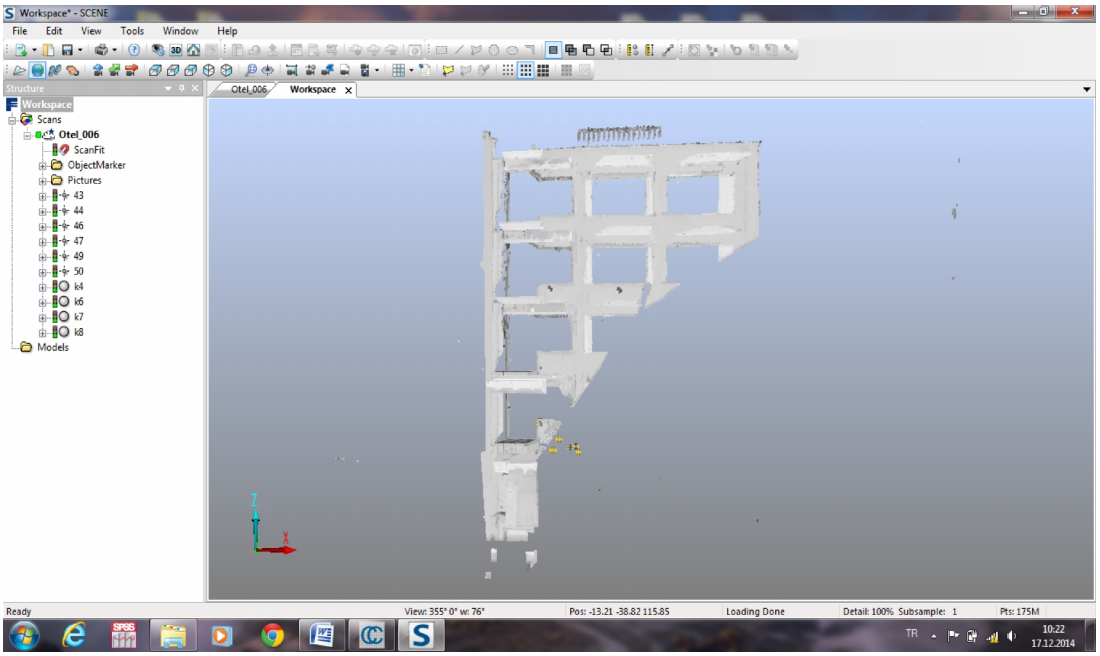
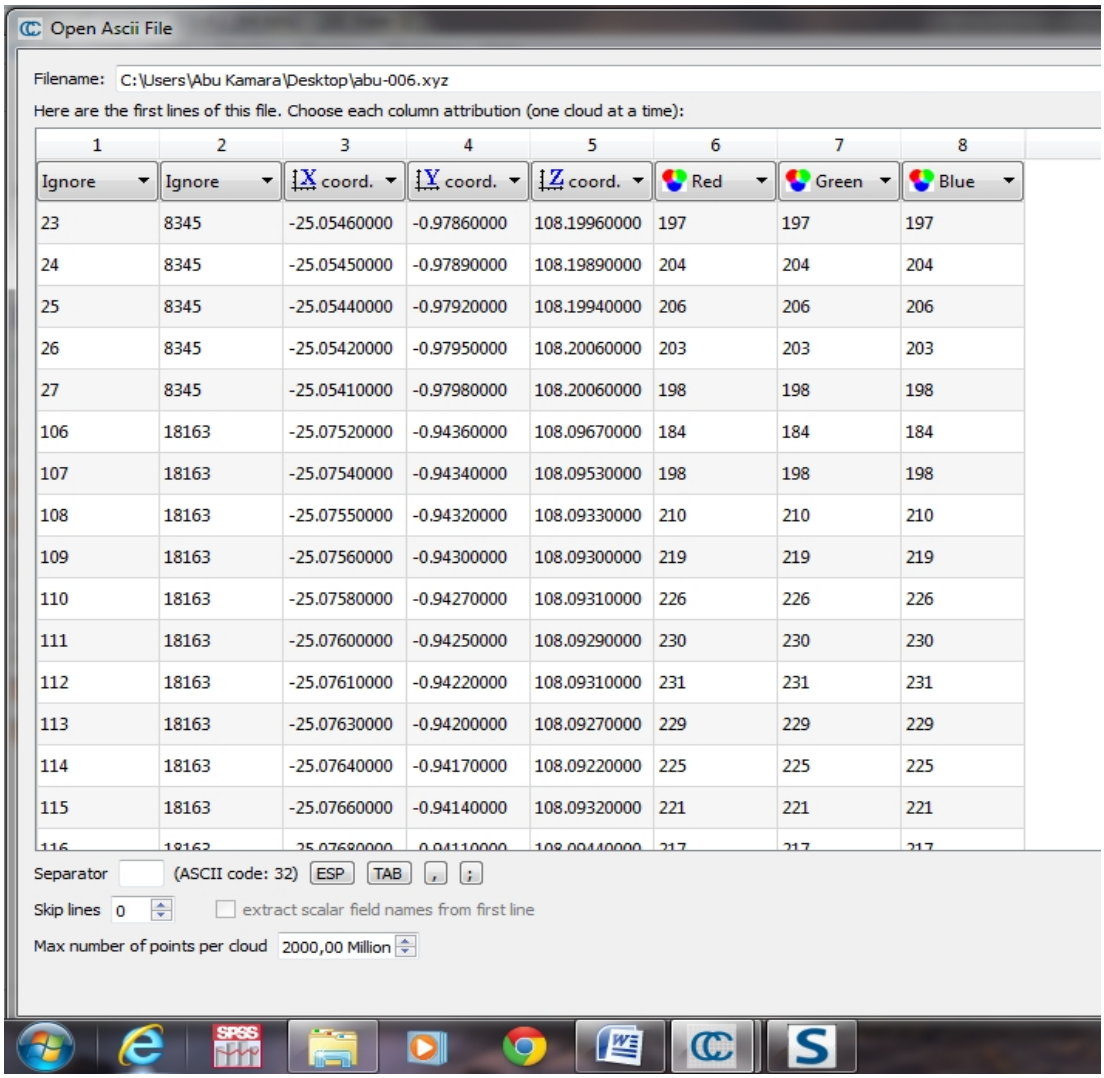


Fig. 5.3. 3D view of the implemented building.

3D view of the building after filteration. The scan coordinates (points) of this surface is in Fig. 5.4. This points were collected from faro scan and saved into Ascii (x, y and z) file format, cloudcompare was used to open the data.



1	2	3	4	5	6	7	8
Ignore	Ignore	X coord.	Y coord.	Z coord.	Red	Green	Blue
23	8345	-25.05460000	-0.97860000	108.19960000	197	197	197
24	8345	-25.05450000	-0.97890000	108.19890000	204	204	204
25	8345	-25.05440000	-0.97920000	108.19940000	206	206	206
26	8345	-25.05420000	-0.97950000	108.20060000	203	203	203
27	8345	-25.05410000	-0.97980000	108.20060000	198	198	198
106	18163	-25.07520000	-0.94360000	108.09670000	184	184	184
107	18163	-25.07540000	-0.94340000	108.09530000	198	198	198
108	18163	-25.07550000	-0.94320000	108.09330000	210	210	210
109	18163	-25.07560000	-0.94300000	108.09300000	219	219	219
110	18163	-25.07580000	-0.94270000	108.09310000	226	226	226
111	18163	-25.07600000	-0.94250000	108.09290000	230	230	230
112	18163	-25.07610000	-0.94220000	108.09310000	231	231	231
113	18163	-25.07630000	-0.94200000	108.09270000	229	229	229
114	18163	-25.07640000	-0.94170000	108.09220000	225	225	225
115	18163	-25.07660000	-0.94140000	108.09320000	221	221	221

Fig 5.4. scan points of 006 surface

Scan 007 in 3D view:

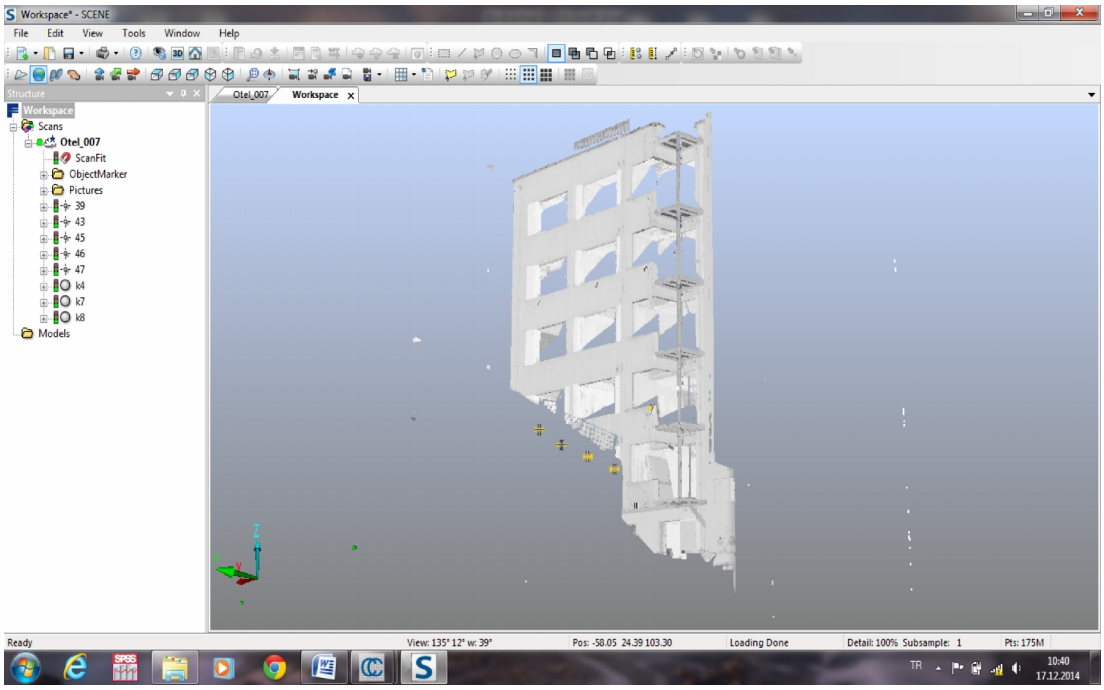
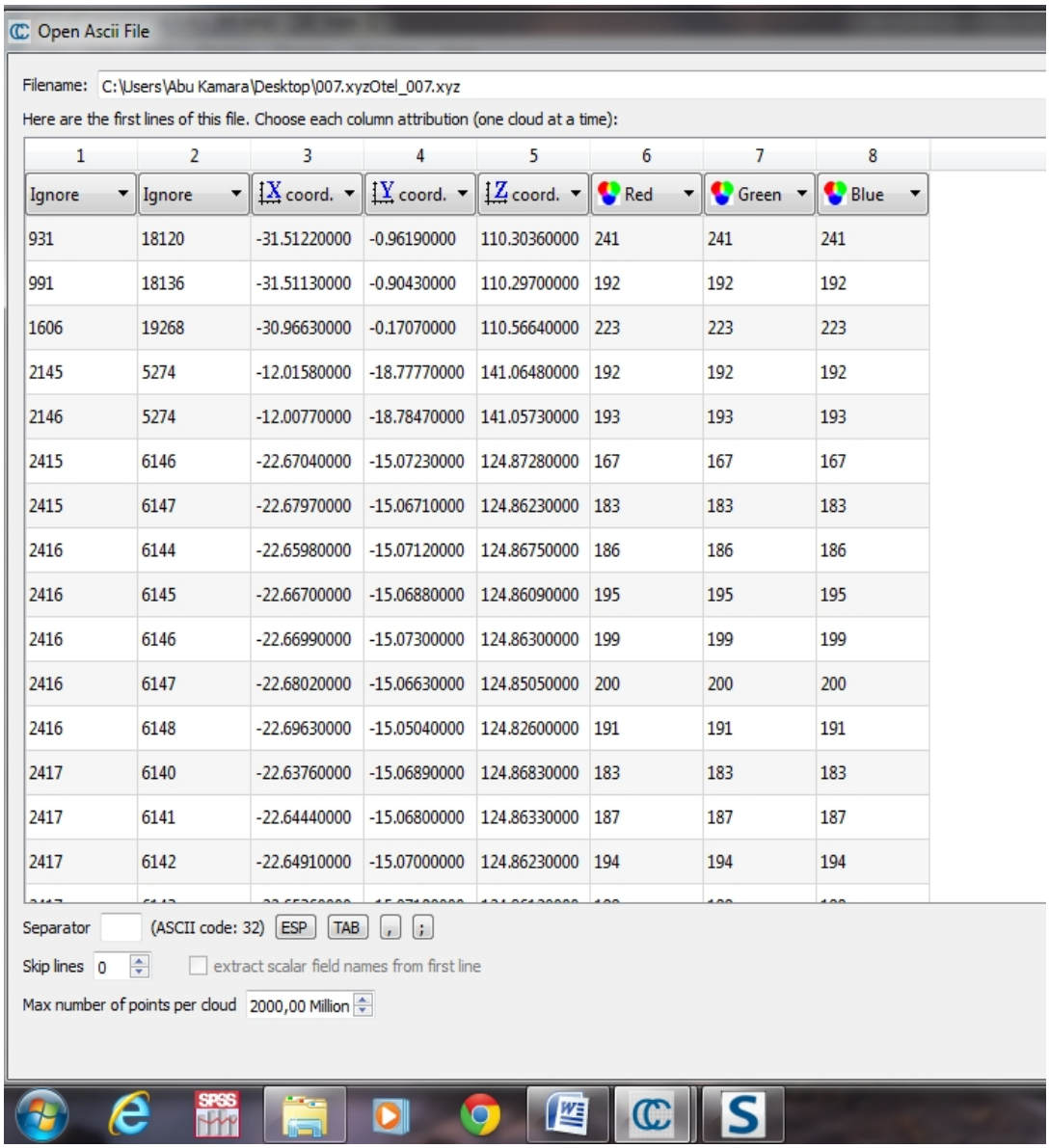


Fig. 5.5. 3D view of the implemented building.

3D view of the building after filteration. The scan coordinates (points) of this surface is in Fig. 5.6. This points were collected from faro scan and saved into Ascii (x, y and z) file format, cloudcompare was used to open the data.



1	2	3	4	5	6	7	8
Ignore	Ignore	X coord.	Y coord.	Z coord.	Red	Green	Blue
931	18120	-31.51220000	-0.96190000	110.30360000	241	241	241
991	18136	-31.51130000	-0.90430000	110.29700000	192	192	192
1606	19268	-30.96630000	-0.17070000	110.56640000	223	223	223
2145	5274	-12.01580000	-18.77770000	141.06480000	192	192	192
2146	5274	-12.00770000	-18.78470000	141.05730000	193	193	193
2415	6146	-22.67040000	-15.07230000	124.87280000	167	167	167
2415	6147	-22.67970000	-15.06710000	124.86230000	183	183	183
2416	6144	-22.65980000	-15.07120000	124.86750000	186	186	186
2416	6145	-22.66700000	-15.06880000	124.86090000	195	195	195
2416	6146	-22.66990000	-15.07300000	124.86300000	199	199	199
2416	6147	-22.68020000	-15.06630000	124.85050000	200	200	200
2416	6148	-22.69630000	-15.05040000	124.82600000	191	191	191
2417	6140	-22.63760000	-15.06890000	124.86830000	183	183	183
2417	6141	-22.64440000	-15.06800000	124.86330000	187	187	187
2417	6142	-22.64910000	-15.07000000	124.86230000	194	194	194

Fig. 5.6. scan points of 007 surface

Scan 008 in 3D view:

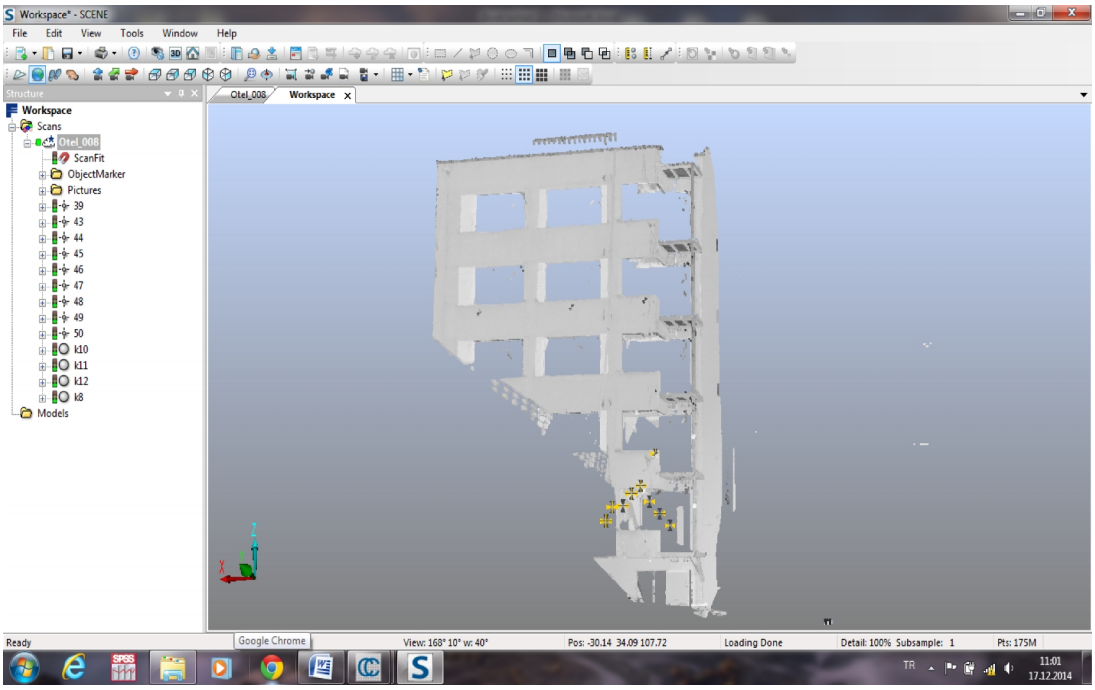


Fig. 5.7. 3D view of the implemented building.

3D view of the building after filteration. The scan coordinates (points) of this surface is in Fig. 5.8. This points were collected from faro scan and saved into Ascii (x, y and z) file format, cloudcompare was used to open the data.

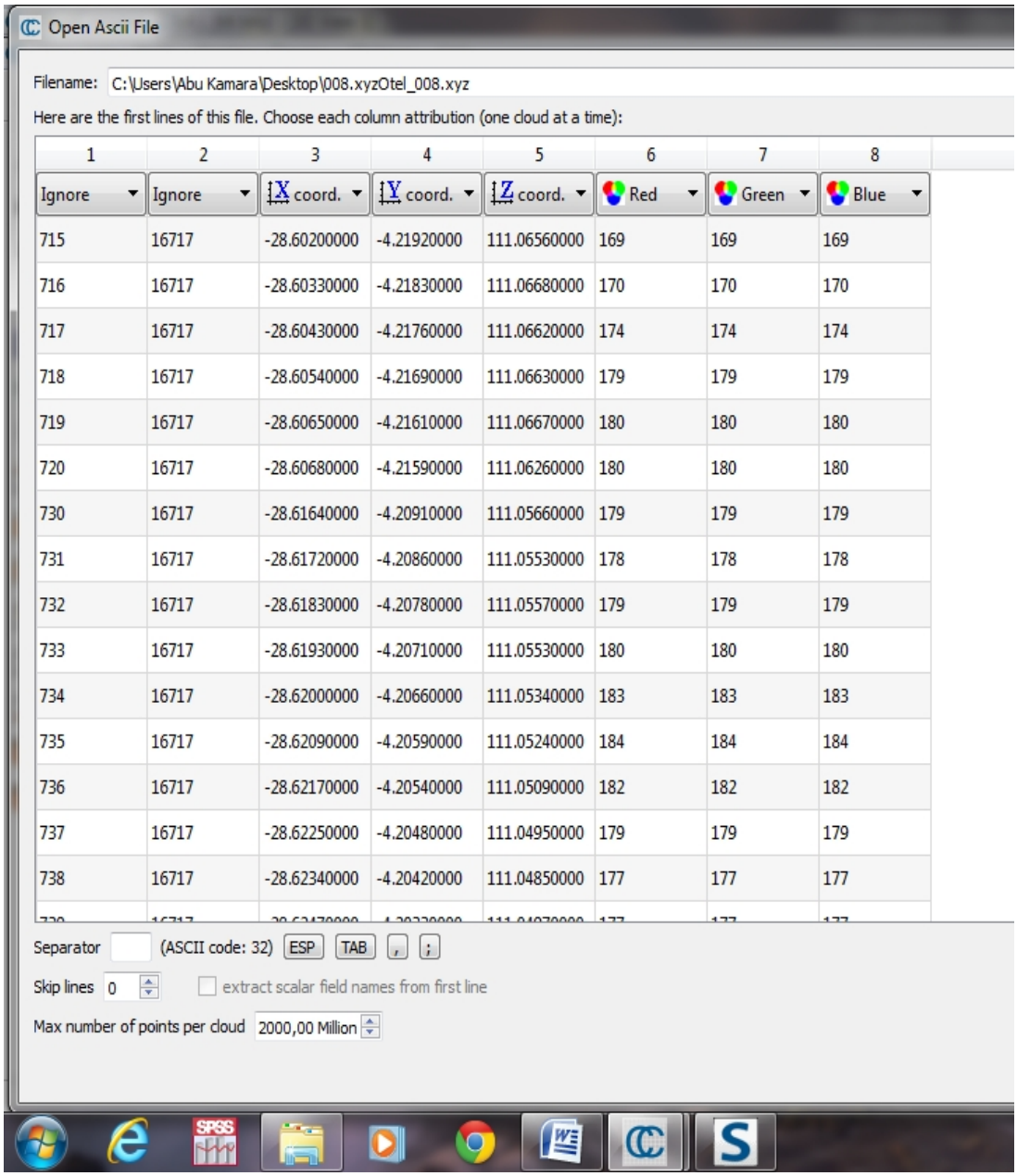


Fig. 5.8. scan points of 008 surface

Scan 009 in 3D view:

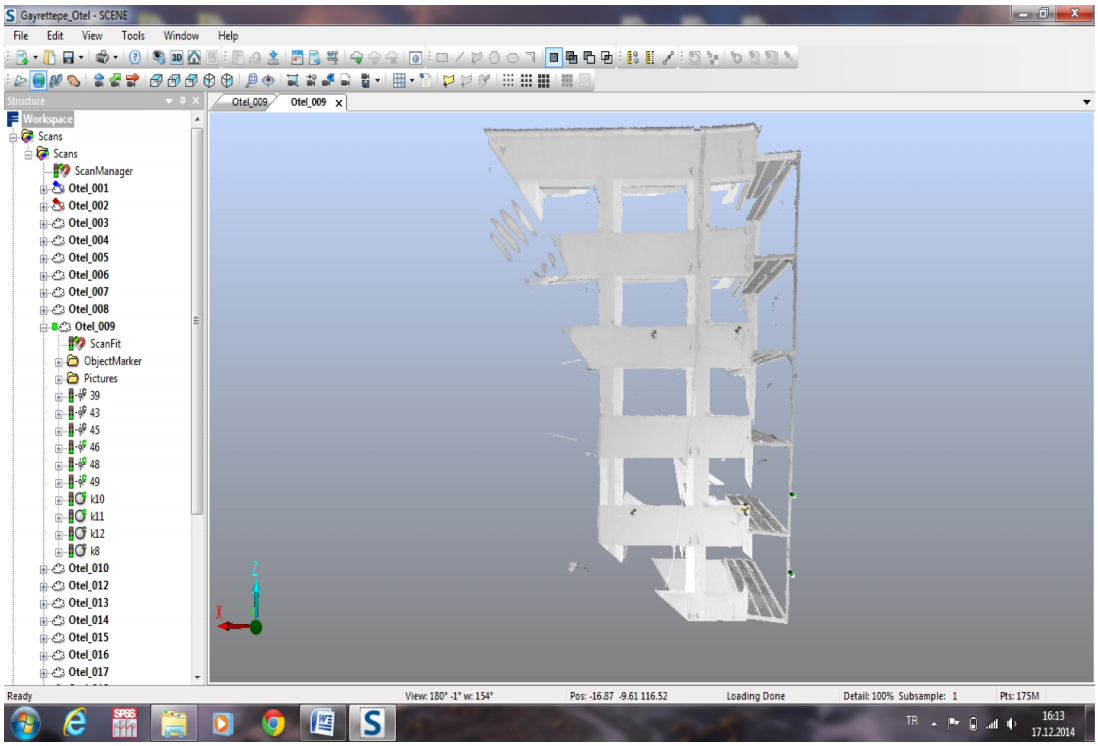


Fig. 5.9. 3D view of the implemented building.

3D view of the building after filteration. The scan coordinates (points) of this surface is in Fig. 5.10. This points were collected from faro scan and saved into Ascii (x, y and z) file format, cloudcompare was used to open the data.

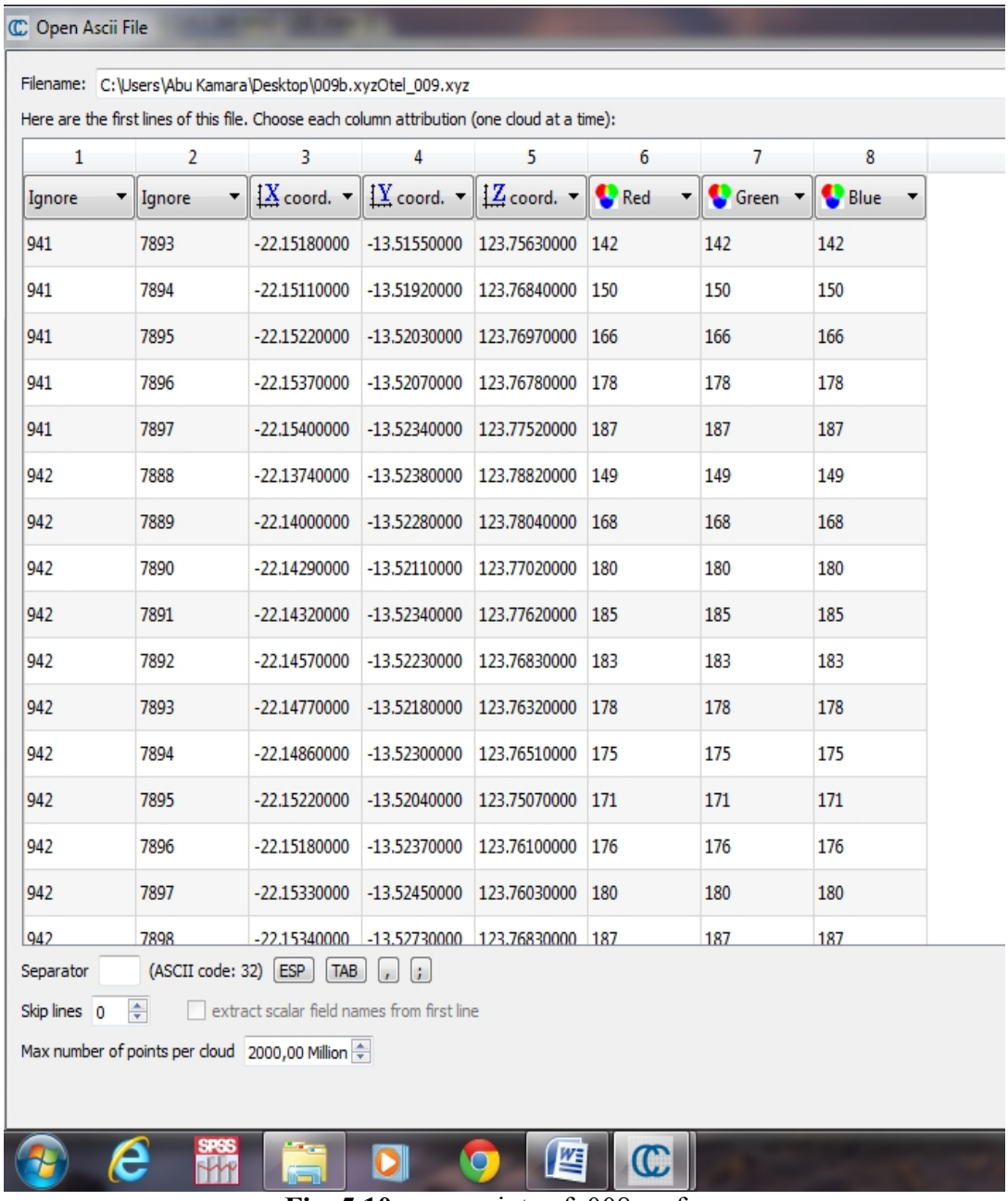


Fig. 5.10. scan points of 008 surface

Control / single cloud point coordinate can also be exported from faro scene in the following file formats VRML files, IGS files and DXF files. The data in these files were identified in Matlab as follow.

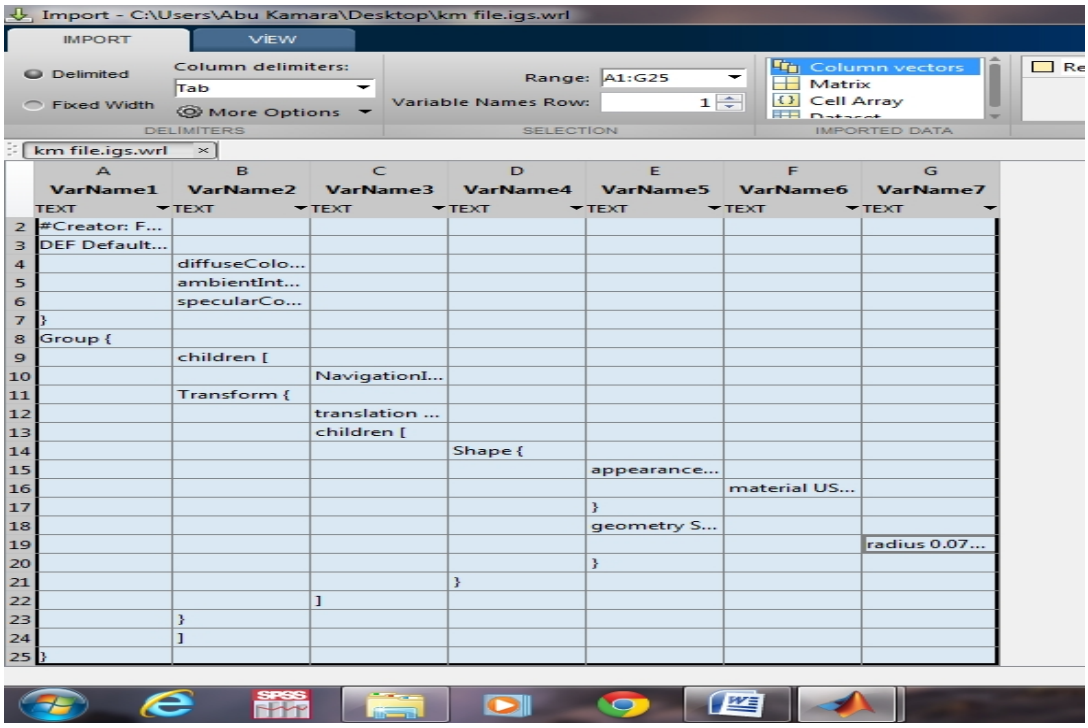


Fig. 5.11. coordinates of K1 (control point) in VRML file format.

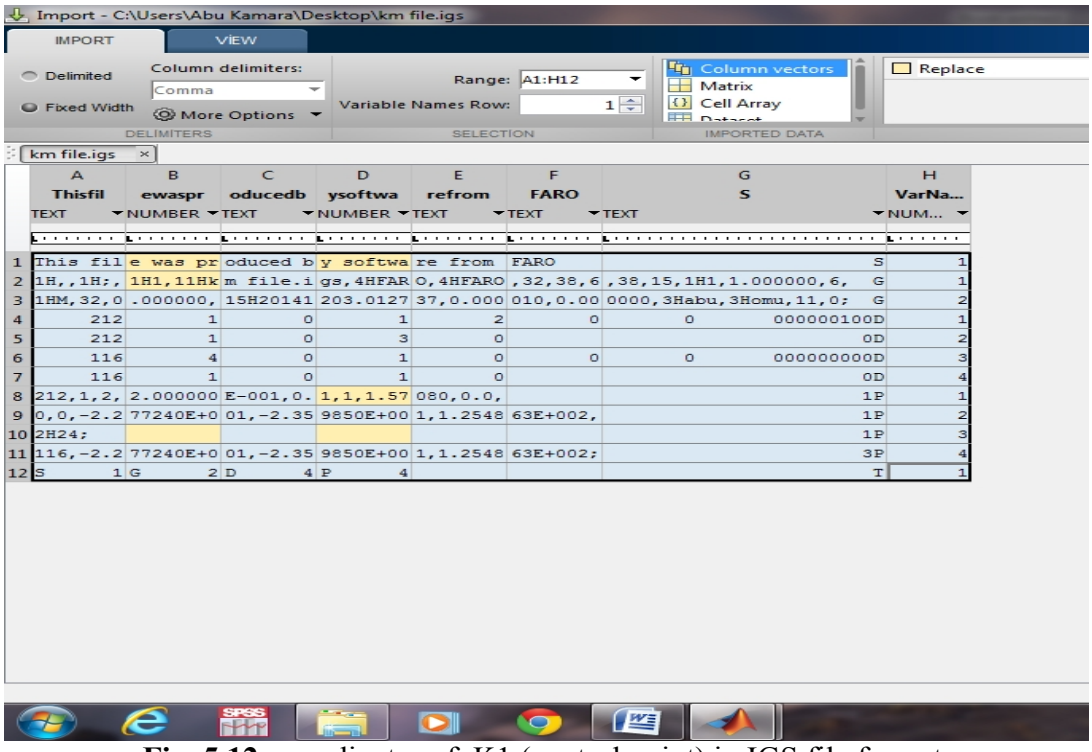


Fig. 5.12. coordinates of K1 (control point) in IGS file format.

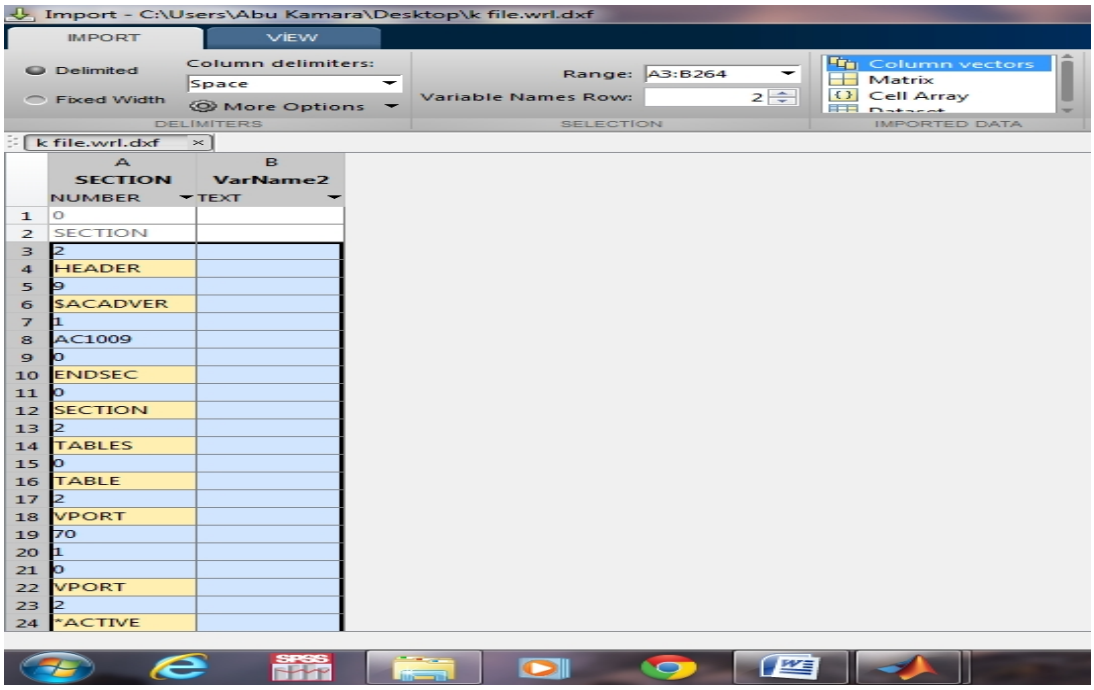


Fig. 5.13. coordinates of K1 (control point) in DXF file format.

As said earlier in section 2.2.1., registration is a pre-processing step required if multiple scans are taken to capture a scene. It aligns and combines multiple data sets into one complete 3D cloud. One of the most popular algorithms is the Iterative Closest Point (ICP) algorithm (Besl and McKay, 1992) which requires an initial rough alignment between two clouds and then iteratively searches for point matches to solve for a transformation. In this thesis, two surfaces (007 and 008) were considered to finely do the alignment. Cloudcompare was used in the transformation process. Figure 5.14. shows the finely registered alignment surfaces in cloudcompare. More detail analysis of such will be shown in our feature studies.

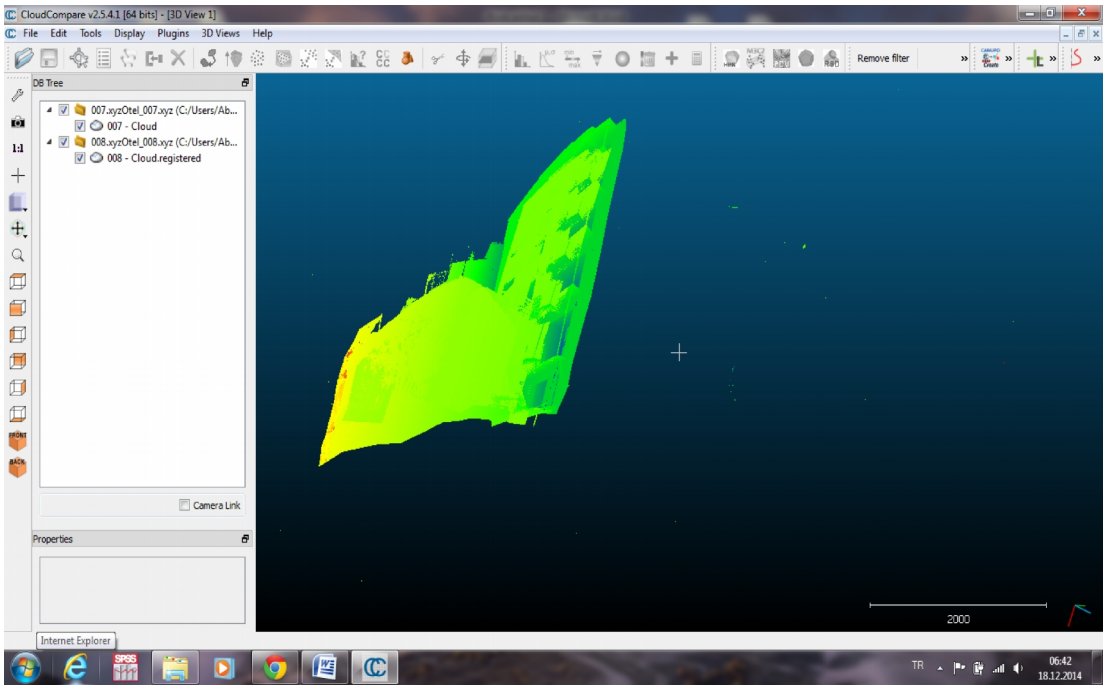


Fig. 5.14. Finely aligned registered surfaces (007 and 008)

6. CONCLUSION

3D model has the advantage over the 2D image, because it creates a more complete picture of the object. Three-dimensional modeling is most often used in areas such as advertising and production.

Three-dimensional modeling is often used for visual presentation of products manufactured by some company. Nowadays no advertising business can work successfully without 3D modeling upscale design activities is also impossible without it.

3D simulation has many advantages. Thus, using 3D models you can hold a variety of optimization of technological processes. Through three-dimensional modeling production efficiency can be significantly increased. Three-dimensional modeling can easily used as a substitute for natural layout.

Using three-dimensional modeling you can clearly evaluate options for joining components and assemblies. Three-dimensional modeling in the design makes it possible to save not only time but also money. At the engineering centers you may order the creation of 3D models according to your drawings, sketches and photographs.

3D modeling is a necessary and very important component of designing process.

3D modeling has the following advantages:

- It can be used to display all possible modifications of the model;
- Allows you to demonstrate the effect of changes in detail;
- Allows you to set precise distances in the model;
- Use it to resize automatically when modifying the model ;
- Helps identify properties to develop a design (namely, mass, volume, moments of inertia, etc.) before the start of production;
- Reduces the number of possible errors in the design stage;
- Accelerates the appearance of the product on the market;
- Assembly design previously executed on a computer, allows an accurate assessment of the interaction of components in the device.

Using 3D modeling, some engineering groups can help you in carrying out the whole design process, as well as engineering analysis and to produce any products of varying complexity and purpose.

3D modeling is very popular in construction industry. Only creating a 3D simulation can provide an analysis of the accuracy of all the systems needed for construction. Without 3D modeling nobody can give 100% assurance that the facility will be safe. Every major architectural and construction project is carried out only when accompanied by 3D modeling. The great advantage of using 3D models is that in this form it is much more easier for a customer to explain his idea. In addition, the presence of errors, 3D model always show them in advance, and, therefore, will have time to correct any deficiencies in the design stage.

3D modeling simplifies the process of harmonization with the client version of the total construction of a facility. 3D models in most cases have a greater effect on the customer than a simple two-dimensional drawings. Three-dimensional model can be done in a very short time from several minutes to several hours. Only a 3D model of the object will provide its rapid design and construction. And the speed of construction in the absence of errors – that's 99% success.

During the studies in this thesis, the three main softwares used in this thesis were observed to have the following drawbacks.

- In Faro scene, we were unable to overlap the picture of scan building into either 3D view, planar view or quick view. For this purpose, an efficient texture mapping routine is required. But however, since the point cloud datasets require huge amount of memory, it is still difficult and seems impossible performing the computations for all of the complete model synchronously. Nowel methods are required to overcome the memory limitation problems.
- Cloudcompare can only shows partial data of scan points in all the selected surfaces. This situation also arises from the memory problems.
- In Matlab, the coordinates of the control points (e.g. **K1, K2**, ...) were not well open to analysis in all the three files formats.

The models especially used for image processing and image understanding tasks, may be generalized to have point cloud data with appropriate generalizations. For future works, we plan to study on the mentioned drawback for finding suitable solutions.

REFERENCES

Abdelmajid, Y., 2012. Investigation and Comparison of 3D Laser Scanning Software Packages. Masters Thesis, Royal Institute of Technology, Stockholm, Sweden.

Abmayr, T., Härtl, F., Mettenleiter, M., Heinz, A., Neumann, B., & Fröhlich, C., 2004. Realistic 3D Reconstruction - Combining Laserscan Data with RGB Color Information, XXth ISPRS Congress, İstanbul.

Ahmad, A. Digital Photogrammetry: An Experience Of Processing Aerial Photograph Of UTM Acquired Using Digital Camera https://www.academia.edu/494079/Digital_Photogrammetry_An_Experience_Of_Processing_Aerial_Photograph_Of_UTM_Acquired_Using_Digital_Camera

Al-Ruzouq, R., 2004. Semi-Automatic Registration of Multi-Source Satellite Imagery with Varying Geometric Resolutions, Doctorial Thesis, University of Calgary, Calgary, Alberta, Canada.

Antolin Sánchez, R., and Brovelli, M. A. 2007. LiDAR Data Filtering with GRASS GIS for the Determination of Digital Terrain Models. Proceedings of Jornadas de SIG Libre, Girona, Espanha.

Armenakis, C., Gao, Y., and Sohn, G., 2012. Semi-automatic Co-registration of Photogrammetric and Lidar Data using Buildings. ISPRS Annals of the Photogrammetry, Remote Sensing and Spatial Information Sciences, XXII ISPRS Congress, Volume I-3, Melbourne, Australia.

Artés, F. LIDAR and Digital Imaging - Multi-Sensor Technology for a Streamlined Digital Environment, Applanix Corporation. http://www.applanix.com/media/downloads/articles_papers/DSS_2005_02_LIDAR-DACS%20Paper.pdf

Avbelj, J., Iwaszczuk, D., Müller, R., Reinartz, P., & Stilla, U., 2013. Line-based Registration of DSM and Hyperspectral Images. International Archives of the Photogrammetry, Remote Sensing and Spatial Information Sciences,Volume XL-1/W1, ISPRS Hannover Workshop, Hannover, Germany.

Axelsson, P., 1999. Processing of laser scanner data—algorithms and applications. ISPRS Journal of Photogrammetry and Remote Sensing, 54(2–3), 138-147. doi: http://dx.doi.org/10.1016/S0924-2716(99)00008-8

Azizi, A., Afsharnia, H., & Hadavand, A., 2013. Evaluation and Analysis of a Parametric Approach for Simultaneous Space Resection-Intersection of High Resolution Satellite Images Without Using Ground Control Points. Paper presented at the International Archives of the Photogrammetry, Remote Sensing and Spatial Information Sciences, Volume XL-1/W3, Tehran, Iran.

Badamikar, N. S., 2014. Automatic Registration of Multiple Texel Images to Form a 3-Dimensional Texel Image. Masters thesis, Utah State University, Logan, Utah.

Badino, H., Huber, D., & Kanade, T., 2011. Integrating LIDAR into Stereo for Fast and Improved Disparity Computation. 3D Imaging, Modeling, Processing, Visualization and Transmission (3DIMPVT), Hangzhou, China.

Basgall, P. L., 2013. Lidar Point Cloud and Stereo Image Point Cloud Fusion. Master of Science in Remote Sensing Intelligence, Masters thesis, Naval Postgraduate School, Monterey, California.

Bornaz, L., & Rinaudo, F., 2004. Terrestrial Laser Scanning Data Processing. XXth ISPRS Congress, Commission, 5, pp. 514–520, İstanbul, Turkey.

Ceesay, L. O., 2014. Reconstructing 3D Building Model from Terrestrial LiDAR Point Cloud, Masters Thesis, National Central University.

Chang, Y.-m., Lai, S.-H., Peng, S.-M., Chang, K.-T., Tu, Y.-S., & Taipei, C., 2008. Data processing of 3D laser scanning on structural deformation. Integrating generations, FIG working week, Stockholm, Sweden.

Conte, G. Performance evaluation of a light weight multi-echo LiDAR for unmanned rotorcraft applications. http://www.int-arch-photogramm-remote-sens-spatial-inf-sci.net/XL-1-W2/87/2013/isprsarchives-XL-1-W2-87-2013.pdf

Deng, F., Minjie, H., & HaiYan, G., 2008. Automatic Registration Between Lidar and Digital Images. In The International Archives of the Photogrammetry, Remote Sensing and Spatial Information Sciences. Vol. XXXVII. Part B1. Beijing 2008, 487-490.

Ergün, B., 2011. Terrestrial Laser Scanning Data Integration in Surveying Engineering. Laser Scanning, Theory and Applications, Prof. Chau-Chang Wang (Ed.), ISBN: 978-953-307-205-0.

Franklin, S., Thomas, S., & Brodeur, M., 2000. Robust Multivariate Outlier Detection Using Mahalanobis' Distance and Modified Stahel-Donoho Estimators. Second International Conference on Establishment Surveys, 697-706, Buffalo, New York.

Ho, H. T., 2009. 3D Surface Matching from Range Images using Multiscale Local Features. Masters Thesis, The University of Adelaide, Australia.

Hoeting, J. A., & Ibrahim, J. G., 1998. Bayesian predictive simultaneous variable and transformation selection in linear model. Journal of Computational Statistics and Data Analysis, 28, 87-103.

İstanbul Büyükşehir Belediyesi., 2007. Fotogrametrik Harita Üretiminde Digital Hava Resim Çekme Makineleri ve Lazer Tarama Yöntemlerinin Kullanım Olanakları Projem İstanbul, Araştırma Projesi. http://katalog.ibb.gov.tr/kutuphane2/YordamVt/projem_istanbul/pi_00003.pdf

Javan, F. D., & Azizi, A., 2008. The Affine Projection Model as a Tool for Rapid Geo-coding of IRS-P5 Satellite Imagery. The International Archives of the Photogrammetry, Remote Sensing and Spatial Information Sciences. Vol. XXXVII. Part B4, Beijing.

Keller, P., Kreylos, O., Vanco, M., Hering-Bertram, M., Cowgill, E., Kellogg, L., Hagen, H., 2011. Extracting and Visualizing Structural Features in Environmental Point Cloud LiDaR Data Sets. In V. Pascucci, X. Tricoche, H. Hagen & J. Tierny (Eds.), Topological Methods in Data Analysis and Visualization (pp. 179-192): Springer Berlin Heidelberg.

Kim, C., 2008. Object-based Integration of Photogrammetric and LIDAR Data for Accurate Reconstruction and Visualization of Building Models. (Doctor of Philosophy), University of Calgary, Calgary, Alberta.

Kim, H., & Hilton, A., 2010. 3d Modelling of Static Environments Using Multiple Spherical Stereo. RMLE Workshop ECCV.

Kim, H., & Hilton, A. 2012. 3D Modelling of Static Environments Using Multiple Spherical Stereo. In K. Kutulakos (Ed.), Trends and Topics in Computer Vision (Vol. 6554, pp. 169-183): Springer Berlin Heidelberg.

Korpela, I., Dahlin, B., Schäfer, H., Bruun, E., Haapaniemi, F., Honkasalo, J., Virtanen, H., 2007. Single-tree forest inventory using lidar and aerial images for 3D treetop positioning, species recognition, height and crown width estimation. ISPRS Workshop on Laser Scanning 2007 and SilviLaser 2007, pp. 227–233 IAPRS XXXVI Part 3 / W52., Espoo, Finland.

Kraus, K., & Rieger, W., 1999. Processing of Laser Scanning Data for Wooded Areas. In FritschD and SpillerR (eds) Photogrammetric Week 1999, Heidelberg, Wichmann: 221–31.

Leberl, F., Irschara, A., Pock, T., Meixner, P., Gruber, M., Scholz, S., & Wiechert, A., 2010. Point clouds: Lidar versus 3d vision. Photogrammetric Engineering and Remote Sensing, 76(10), 1123–1134.

Lidar 101:, 2012. An Introduction to Lidar Technology, Data and Applications. http://coast.noaa.gov/digitalcoast/_/pdf/lidar101.pdf

Litke, N., Droske, M., Rumpf, M., & Schröder, P., 2005. An Image Processing Approach to Surface Matching. Eurographics Symposium on Geometry Processing Vienna, Austria.

Meng, X., Currit, N., & Zhao, K., 2010. Ground Filtering Algorithms for Airborne LiDAR Data: A Review of Critical Issues. Remote Sensing, 2(3), 833-860. doi: doi:10.3390/rs2030833

Miqdad, A. A.-A., 2012. The Role of Mother Tongue in Reception and Production of Collocations by English Majors at the Palestinian Universities. Masters thesis, The Islamic University of Gaza.

Mitsakaki, C., 2004. Coordinate Transformations. FIG Working Week, Athens, Grace.

Murphy, M., McGovern, E., & Pavia, S., 2006. The Processing of Laser Scan Data for the Analysis of Historic Structures in Ireland. The 7th International Symposium on Virtual Reality, Archaeology and Cultural Heritage VAST.

Ok, A. Ö., Wegner, J. D., Heipke, C., Rottensteiner, F., Sörgel, U., & Toprak, V., 2010. Çok Bantlı Stereo Hava Fotoğraflarından Doğrusal Çizgilerin Otomatik Geri-Çatımı için Yeni Bir Yaklaşım. III. Uzaktan Algılama ve Coğrafi Bilgi Sistemleri Sempozyumu, Gebze, Kocaeli.

Riegl, J., Studnicka, N., & Ullrich, A., 2003. Merging and processing of laser scan data and high-resolution digital images acquired with a hybrid 3D laser sensor. Proceedings of CIPA XIX international symposium, Commission V, WG5, Antalya.

Salzmann, M., 2009. Learning and Recovering 3D Surface Deformations, Doctorial thesis, Ecole Polytechnique Federale de Lausanne, Suisse.

Schenk, T., 2005. Introduction to Photogrammetry. The Ohio State University, Columbus, OH.

Schenk, T., & Csathó, B., 2002. Fusion of Lidar data and aerial imagery for a more complete surface description, pp. A-310 ff. ISPRS. Photogrammetr. Comput. Vision, Graz, Austria.

Sietz, S. M., 1997. Image-based Transformation of Viewpoint and Scene Appearance. Doctorial Thesis, University of Wisconsin.

St-Onge, B. A., & Achaichia, N., 2001. Measuring forest canopy height using a combination of lidar and aerial photography data. International Archives of Photogrammetry and Remote Sensing, XXXIV-3/W4, pp. 131–137, Annapolis, MD.

Staiger, R. Terrestrial Laser Scanning Technology, Systems and Applications https://www.fig.net/pub/morocco/proceedings/TS12/TS12_3_staiger.pdf

Syed, S., Dare, P., & Simon, J., 2005. Semi-automatic 3D Building Model Generation From Lidar and High Resolution Imagery. SSC2005 Spatial Intelligence, Innovation and Praxis: The national biennial Conference of the Spatial Sciences Institute, September, 2005, Melbourne Special Science Institute.

Şehsuvaroğlu, M. S., Eker, O., Erdoğan, M., ve Yıldız, F., 2014. Sayısal Yüzey Modeli Üretiminde Fotogrametri mi, LiDAR mı? . Harita Dergisi, Sayı 151, Ocak.

Taati, B., 2009. Generation and Optimization of Local Shape Descriptors for Point Matching in 3-D Surfaces. Doctorial Thesis, Queen's University, Kingston, Ontario, Canada.

Theory and practice on Terrestrial Laser Scanning, Training material based on practical applications Version 4., 2008.

Toth, C. K., and Grejner-Brezezinska, D. A., 2000. Complementarity of LIDAR and Stereo Imagery for Enhanced Surface Extraction. International Archive of Photogrammetry and Remote Sensing. v. XXXIII, Part B3, Amsterdam.

Valadan Zoej, M. J., & Sadeghian, S. Rigorous and Non-Rigorous Photogrammetric Processing of Ikonos Geo Image.

Walsh, S. B., & Hajjar, J. F., 2009. Data Processing of Laser Scans Towards Applications in Structural Engineering NSEL Report Series. Urbana, IL: Department of Civil and Environmental Engineering University of Illinois at Urbana-Champaign.

Yıldız, F., 2010. Dijital (Sayısal) Fotogrametri Teknolojisi. Coğrafi Bilgi Teknolojileri Çalıştayı, "Akademik Perspektif", Cebit Bilişim Zirvesi, Beylikdüzü, İstanbul.

Yogeswaran, A., & Payeur, P., 2012. 3D Surface Analysis for Automated Detection of Deformations on Automative Body Panels. New Advances in Vehicular Technology and Automotive Engineering, ISBN 978-953-51-0698-2. doi: http://dx.doi.org/10.5772/45790

Yoshiyasu, Y., Yoshida, E., Yokoi, K., & Sagawa, R., 2014. Symmetry-Aware Nonrigid Matching of Incomplete 3D Surfaces. Computer Vision and Pattern Recognition (CVPR), 2014 IEEE Conference on.

CURRICULUM VITAE



PERSONAL DETAILS:

NAME:	Abu KAMARA
DATE OF BIRTH:	8Th February, 1985
PLACE OF BIRTH:	Pujehun –Southern Sierra Leone
MARITAL STATUS:	Single
NATIONALITY:	Sierra Leonean
SEX:	Male
LANGUAGE SPOKEN:	English, Turkish, Kiro and Mende
CONTACT ADDRESS:	Altunizade Mah. İnci Çikmazi, inci sitesi D.3 Blok D.7 Üsküdar
CONTACT NUMBER:	+90 (541) 925 02 89
E-MAIL ADDRESS:	abukamara@geocad.com.tr motifharita4@hotmail.com
CAREER INTEREST:	Geomatics Engineering / Geology

EDUCATIONAL BACKGROUND:

2013-2015	Masters of Science (MSc) / Geomatics Engineering, Ondokuz Mayıs University-Samsun / Turkey.
2006-2009	Bachelor of Science (Bsc) Geology, Fourah Bay College,University of Sierra Leone.
2000-2003	WASSCE Ahmadiyya Muslim Secondary School, Bo / Sierra Leone.
2012-2013	TÖMER, ANKARA University Kadıköy Branch -İstanbul / TURKEY .

PROJECTS

PERIOD	**WORK AND INSTITUTION**
2014 (February-May)	Academic Seminar , Ondokuz Mayıs University, Geomatics Engineerig Department- Samsun/TURKEY

TOPIC:

3D Surface Registration: Matching Of The Corresponding (common) Points And Computation Of The Transformation Function Between Surfaces

PERIOD	**WORK AND INSTITUTION**
2014 -2015	Thesis, Ondokuz Mayıs University, Geomatics Engineerig Department - Samsun/TURKEY

TOPIC:

3D Reconstructıon Of Point Clouds And Solid Models From Lidar And Digital Stereo Images

AIMS:

Creating 3D reconstruction of Point Clouds and Solid Models from LİDAR and Digital Stereo Images using a building as a case study. Ground Based-LİDAR as one of the instrument of LİDAR technology was used as a method. FARO scanner was used in the scanning processed. FARO scene, Matlab, Cloudcompare and many more software were used in the registration processes and analysis of the data.

INTERNSHIP

PERIOD, POSITION, INSTITUTION / AGENCY:	
2010-2012	Trainee Geomatics Engineer at Borat Sayısal Haritacılık Sistemleri (GeoCAD), İstanbul / Turkey.

EXPERIENCES:

- Mapping 250km rail way from Denizli / Sandıklı-TURKEY
- Survey of Benze Gas – İstanbul / TURKEY
- Surveying of feature road construction-Eskişehir / TURKEY

2008-2009 Geologist at the Canaf Diamond Mining Company, Baoma Chiefdom / Bo District, Southern Sierra Leone.

EXPERIENCE:

- Analysing mining activities and exploring for diamond deposits.

TRANSFERABLE SKILLS:

- Translation of journals from either English to Turkish or from Turkish to English.
- Use of software like FARO scene, CloudCompare, QT- Quick Terrain Modeler[8] Agisoft, ArcGIS ,GeoCAD, and many more for the interpretation / production of maps after collections and inputing of data.
- GPS Navigation

WORKSHOP **PLACE**

October, 2014 (20-24) Ondokuz Mayıs University -Samsun / TURKEY, Agricultural Department seminar salon

TOPIC

Entrepreneurship research with data from global entrepreneurship monitor

April, 2011 (25-29) Congress center of general directorate of MTA, Ankara- TURKEY.

64th Geological Congress of TURKEY

April, 2011 (18-22) Sheraton Hotel -Ankara / TURKEY

TMMOB Chambers of Mapping and Cadastre Engineers 13th Turkish Mapping, Scientific and Technical Congress.

LEADERSHIP QUALITY

2014-present, President of the African Students Association at Ondokuz Mayıs University (OMU) - Samsun / TURKEY.

Roles

- Intermediary between African Students at OMU and the Administrave Board of the university.
- Creating an easy flow of communications amoung African Students at OMU.
- African Students coming together to discuss our academic problems faces in our various departments and finding a way forward.
- Creating a platform wherein African Students can come together and socialize, vice versa showing our various cultures.
- Being our brothers and sisters keepers, that is, if any of our member is seriously ill the person closer to him or her should let the committe know inorder to help the person to sick suitable medical attention.

HOBBIES

- Reading of scientific Journals
- Foreign Cultures
- Sports (Foot Ball, Basket Ball, Volley Ball and Table Tennis)
- Socializing